

Appendix 3.N

Intentionally Deleted

|

Appendix 3.0

Intentionally Deleted

Appendix 3.P

Intentionally Deleted

Appendix 3.Q

Intentionally Deleted

|

Appendix 3.R

Intentionally Deleted

Appendix 3.S

Intentionally Deleted

Appendix 3.T

Intentionally Deleted

|

APPENDIX 3.U: HI-STORM 100 COMPONENT THERMAL EXPANSIONS; MPC-24

3.U.1 Scope

In this calculation, estimates of operating gaps, both radially and axially, are computed for the fuel basket-to-MPC shell, and for the MPC shell-to-overpack. This calculation is in support of the results presented in Section 3.4.4.2.

3.U.2 Methodology

Bounding temperatures are used to construct temperature distributions that will permit calculation of differential thermal expansions both radially and axially for the basket-to-MPC gaps, and for the MPC-to-overpack gaps. Reference temperatures are set at 70°F for all components. Temperature distributions are computed at the hottest cross section of the HI-STORM 100. A comprehensive nomenclature listing is provided in Section 3.U.6.

3.U.3 References

[3.U.1] Boley and Weiner, Theory of Thermal Stresses, John Wiley, 1960, Sec. 9.10, pp. 288-291.

[3.U.2] Burgreen, Elements of Thermal Stress Analysis, Arcturus Publishers, Cherry Hill NJ, 1988.

3.U.4 Calculations for Hot Components (Middle of System)

3.U.4.1 Input Data

Based on thermal calculations in Chapter 4, the following temperatures are appropriate at the hottest location of the cask (see Figure 3.U.1 and Tables 4.4.9 and 4.4.36).

The temperature change at the overpack inner shell, $\Delta T_{1h} := 199 - 70$	
The temperature change at the overpack outer shell, $\Delta T_{2h} := 145 - 70$	
The temperature change at the mean radius of the MPC shell, $\Delta T_{3h} := 344 - 70$	
The temperature change at the outside of the MPC basket, $\Delta T_{4h} := (486 - 70) \cdot 1.1$	
The temperature change at the center of the basket (helium gas), $\Delta T_{5h} := 650 - 70$	

Note that the outer basket temperature is conservatively amplified by 10% to insure a bounding parabolic distribution. This conservatism serves to maximize the growth of the basket. The geometry of the components are as follows (referring to Figure 3.U.1)

The outer radius of the overpack, $b := 66.25 \cdot \text{in}$

The minimum inner radius of the overpack, $a := 34.75 \cdot \text{in}$

The mean radius of the MPC shell, $R_{\text{mpc}} := \frac{68.375 \cdot \text{in} - 0.5 \cdot \text{in}}{2}$ $R_{\text{mpc}} = 33.938 \text{ in}$

The initial MPC-to-overpack radial clearance, $RC_{\text{mo}} := .5 \cdot (69.5 - 68.5) \cdot \text{in}$

$$RC_{\text{mo}} = 0.5 \text{ in}$$

This initial radial clearance value, used to perform a radial growth check, is conservatively based on the channel radius (see Dwg. 1495, Sh. 5) and the maximum MPC diameter. For axial growth calculations for the MPC-to-overpack lid clearance, the axial length of the overpack is defined as the distance from the top of the pedestal platform to the bottom of the lid bottom plate, and the axial length of the MPC is defined as the overall MPC height.

The axial length of the overpack, $L_{\text{ovp}} := 191.5 \cdot \text{in}$

The axial length of the MPC, $L_{\text{mpc}} := 190.5 \cdot \text{in}$

The initial MPC-to-overpack nominal axial clearance, $AC_{\text{mo}} := L_{\text{ovp}} - L_{\text{mpc}}$

$$AC_{\text{mo}} = 1 \text{ in}$$

For growth calculations for the fuel basket-to-MPC shell clearances, the axial length of the basket is defined as the total length of the basket and the outer radius of the basket is defined as the mean radius of the MPC shell minus one-half of the shell thickness minus the initial basket-to-shell radial clearance.

The axial length of the basket, $L_{\text{bas}} := 176.5 \cdot \text{in}$

The initial basket-to-MPC lid nominal axial clearance, $AC_{\text{bm}} := 1.8125 \cdot \text{in}$

The initial basket-to-MPC shell nominal radial clearance, $RC_{\text{bm}} := 0.1875 \cdot \text{in}$

The outer radius of the basket, $R_b := R_{\text{mpc}} - \frac{0.5}{2} \cdot \text{in} - RC_{\text{bm}}$ $R_b = 33.5 \text{ in}$

The coefficients of thermal expansion used in the subsequent calculations are based on the mean temperatures of the MPC shell and the basket (conservatively estimated high).

The coefficient of thermal expansion for the MPC shell, $\alpha_{\text{mpc}} := 9.015 \cdot 10^{-6}$

The coefficient of thermal expansion for the basket, $\alpha_{\text{bas}} := 9.60 \cdot 10^{-6}$ 600 deg. F

3.U.4.2 - Thermal Growth of the Overpack

Results for thermal expansion deformation and stress in the overpack are obtained here. The system is replaced by a equivalent uniform hollow cylinder with approximated average properties.

Based on the given inside and outside surface temperatures, the temperature solution in the cylinder is given in the form:

$$C_a + C_b \cdot \ln\left(\frac{r}{a}\right)$$

where

$$C_a := \Delta T_{1h} \quad C_a = 129$$

$$C_b := \frac{\Delta T_{2h} - \Delta T_{1h}}{\ln\left(\frac{b}{a}\right)} \quad C_b = -83.688$$

Next, form the integral relationship:

$$\text{Int} := \int_a^b \left[C_a + C_b \cdot \ln\left(\frac{r}{a}\right) \right] \cdot r \, dr$$

The Mathcad program, which was used to create this appendix, is capable of evaluating the integral "Int" either numerically or symbolically. To demonstrate that the results are equivalent, the integral is evaluated both ways in order to qualify the accuracy of any additional integrations that are needed.

The result obtained through numerical integration, $\text{Int} = 1.533 \times 10^5 \text{ in}^2$

To perform a symbolic evaluation of the solution the integral "Ints" is defined. This integral is then evaluated using the Maple symbolic math engine built into the Mathcad program as:

$$\text{Int}_s := \int_a^b \left[C_a + C_b \cdot \ln\left(\frac{r}{a}\right) \right] \cdot r \, dr$$

$$\text{Int}_s := \frac{1}{2} \cdot C_b \cdot \ln\left(\frac{b}{a}\right) \cdot b^2 + \frac{1}{2} \cdot C_a \cdot b^2 - \frac{1}{4} \cdot C_b \cdot b^2 + \frac{1}{4} \cdot C_b \cdot a^2 - \frac{1}{2} \cdot C_a \cdot a^2$$

$$\text{Int}_s = 1.533 \times 10^5 \text{ in}^2$$

We note that the values of Int and Ints are identical. The average temperature in the overpack cylinder (T_{bar}) is therefore determined as:

$$T_{\text{bar}} := \frac{2}{(b^2 - a^2)} \cdot \text{Int} \qquad T_{\text{bar}} = 96.348$$

We estimate the average coefficient of thermal expansion for the overpack by weighting the volume of the various layers. A total of four layers are identified for this calculation. They are:

- 1) the inner shell
- 2) the shield shell
- 3) the radial shield
- 4) the outer shell

Note that the shield shell was removed from the HI-STORM 100 design as of 6/01. The replacement of the shield shell with concrete, however, has a negligible effect on the resultant coefficient of thermal expansion because (a) the difference in thermal expansion coefficients between concrete and carbon steel is small and (b) the shield shell accounts for a small percentage of the total overpack radial thickness.

Thermal properties are based on estimated temperatures in the component and coefficient of thermal expansion values taken from the tables in Chapter 3. The following averaging calculation involves the thicknesses (t) of the various components, and the estimated coefficients of thermal expansion at the components' mean radial positions. The results of the weighted average process yields an effective coefficient of linear thermal expansion for use in computing radial growth of a solid cylinder (the overpack).

The thicknesses of each component are defined as:

$$t_1 := 1.25 \text{ in}$$

$$t_2 := 0.75 \text{ in}$$

$$t_3 := 26.75 \text{ in}$$

$$t_4 := 0.75 \text{ in}$$

and the corresponding mean radii can therefore be defined as:

$$r_1 := a + .5 t_1 + 2.0 \text{ in} \qquad \text{(add the channel depth)}$$

$$r_2 := r_1 + .5 t_1 + .5 t_2$$

$$r_3 := r_2 + .5 \cdot t_2 + .5 \cdot t_3$$

$$r_4 := r_3 + .5 \cdot t_3 + .5 \cdot t_4$$

To check the accuracy of these calculations, the outer radius of the overpack is calculated from r_4 and t_4 , and the result is compared with the previously defined value (b).

$$b_1 := r_4 + 0.5 \cdot t_4$$

$$b_1 = 66.25 \text{ in}$$

$$b = 66.25 \text{ in}$$

We note that the calculated value b_1 is identical to the previously defined value b . The coefficients of thermal expansion for each component, estimated based on the temperature gradient, are defined as:

$$\alpha_1 := 5.782 \cdot 10^{-6}$$

$$\alpha_2 := 5.782 \cdot 10^{-6}$$

$$\alpha_3 := 5.5 \cdot 10^{-6}$$

$$\alpha_4 := 5.638 \cdot 10^{-6}$$

Thus, the average coefficient of thermal expansion of the overpack is determined as:

$$\alpha_{\text{avg}} := \frac{r_1 \cdot t_1 \cdot \alpha_1 + r_2 \cdot t_2 \cdot \alpha_2 + r_3 \cdot t_3 \cdot \alpha_3 + r_4 \cdot t_4 \cdot \alpha_4}{\frac{a+b}{2} \cdot (t_1 + t_2 + t_3 + t_4)}$$

$$\alpha_{\text{avg}} = 5.628 \times 10^{-6}$$

Reference 3.U.1 gives an expression for the radial deformation due to thermal growth. At the inner radius of the overpack ($r = a$), the radial growth is determined as:

$$\Delta R_{\text{ah}} := \alpha_{\text{avg}} \cdot a \cdot T_{\text{bar}}$$

$$\Delta R_{\text{ah}} = 0.019 \text{ in}$$

Similarly, an overestimate of the axial growth of the overpack can be determined by applying the average temperature (T_{bar}) over the entire length of the overpack as:

$$\Delta L_{\text{ovph}} := L_{\text{ovp}} \cdot \alpha_{\text{avg}} \cdot T_{\text{bar}}$$

$$\Delta L_{\text{ovph}} = 0.104 \text{ in}$$

Estimates of the secondary thermal stresses that develop in the overpack due to the radial temperature variation are determined using a conservatively high value of E as based on the temperature of the steel. The circumferential stress at the inner and outer surfaces (σ_{ca} and σ_{cb} , respectively) are determined as:

The Young's Modulus of the material, $E := 28300000 \cdot \text{psi}$

$$\sigma_{ca} := \alpha_{avg} \cdot \frac{E}{a^2} \left[2 \cdot \frac{a^2}{(b^2 - a^2)} \cdot \text{Int} - (C_a) \cdot a^2 \right]$$

$$\sigma_{ca} = -5200 \text{ psi}$$

$$\sigma_{cb} := \alpha_{avg} \cdot \frac{E}{b^2} \left[2 \cdot \frac{b^2}{(b^2 - a^2)} \cdot \text{Int} - \left[C_a + C_b \cdot \left(\ln \left(\frac{b}{a} \right) \right) \right] \cdot b^2 \right]$$

$$\sigma_{cb} = 3400 \text{ psi}$$

The radial stress due to the temperature gradient is zero at both the inner and outer surfaces of the overpack. The radius where a maximum radial stress is expected, and the corresponding radial stress, are determined by trial and error as:

$$N := 0.37$$

$$r := a \cdot (1 - N) + N \cdot b$$

$$r = 46405 \text{ in}$$

$$\sigma_r := \alpha_{avg} \cdot \frac{E}{r^2} \left[\frac{r^2 - a^2}{2} \cdot T_{bar} - \int_a^r \left[C_a + C_b \cdot \left(\ln \left(\frac{y}{a} \right) \right) \right] \cdot y \, dy \right]$$

$$\sigma_r = -678201 \text{ psi}$$

The axial stress developed due to the temperature gradient is equal to the sum of the radial and tangential stresses at any radial location. (see eq. 9.10.7) of [3.U.1]. Therefore, the axial stresses are available from the above calculations. The stress intensities in the overpack due to the temperature distribution are below the Level A membrane stress.

3.U.4.3 Thermal Growth of the MPC Shell

The radial and axial growth of the MPC shell (ΔR_{mpch} and ΔL_{mpch} , respectively) are determined as:

$$\Delta R_{mpch} := \alpha_{mpc} \cdot R_{mpc} \cdot \Delta T_{3h} \quad \Delta R_{mpch} = 0.084 \text{ in}$$

$$\Delta L_{mpch} := \alpha_{mpc} \cdot L_{mpc} \cdot \Delta T_{3h} \quad \Delta L_{mpch} = 0.471 \text{ in}$$

3.U.4.4 Clearances Between the MPC Shell and Overpack

The final radial and axial MPC shell-to-overpack clearances (RG_{moh} and AG_{moh} , respectively) are determined as:

$$RG_{moh} := RC_{mo} + \Delta R_{ah} - \Delta R_{mpch}$$

$$RG_{moh} = 0.435 \text{ in}$$

$$AG_{moh} := AC_{mo} + \Delta L_{ovph} - \Delta L_{mpch}$$

$$AG_{moh} = 0.633 \text{ in}$$

Note that this axial clearance (AG_{moh}) is based on the temperature distribution at the hottest cross section.

3.U.4.5 Thermal Growth of the MPC-24 Basket

Using formulas given in [3.U.2] for a solid body of revolution, and assuming a parabolic temperature distribution in the radial direction with the center and outer temperatures given previously, the following relationships can be developed for free thermal growth.

$$\text{Define } \Delta T_{bas} := \Delta T_{5h} - \Delta T_{4h} \quad \Delta T_{bas} = 122.4$$

$$\text{Then the mean temperature can be defined as } T_{bar} := \frac{2}{R_b^2} \int_0^{R_b} \left(\Delta T_{5h} - \Delta T_{bas} \cdot \frac{r^2}{R_b^2} \right) \cdot r \, dr$$

Using the Maple symbolic engine again, the closed form solution of the integral is:

$$T_{\text{bar}} := \frac{2}{R_b^2} \left(\frac{-1}{4} \cdot \Delta T_{\text{bas}} \cdot R_b^2 + \frac{1}{2} \cdot \Delta T_{5\text{H}} \cdot R_b^2 \right)$$

$$T_{\text{bar}} = 518.8$$

The corresponding radial growth at the periphery (ΔR_{bh}) is therefore determined as:

$$\Delta R_{\text{bh}} := \alpha_{\text{bas}} \cdot R_b \cdot T_{\text{bar}} \quad \Delta R_{\text{bh}} = 0.167 \text{ in}$$

and the corresponding axial growth (ΔL_{bas}) is determined from [3.U.2] as:

$$\Delta L_{\text{bh}} := \Delta R_{\text{bh}} \cdot \frac{L_{\text{bas}}}{R_b}$$

$$\Delta L_{\text{bh}} = 0.879 \text{ in}$$

Note that the coefficient of thermal expansion for the hottest basket temperature has been used, and the results are therefore conservative.

3.U.4.6 Clearances Between the Fuel Basket and MPC Shell

The final radial and axial fuel basket-to-MPC shell and lid clearances (RG_{bmh} and AG_{bmh} , respectively) are determined as:

$$RG_{\text{bmh}} := RC_{\text{bm}} - \Delta R_{\text{bh}} + \Delta R_{\text{mpch}}$$

$$RG_{\text{bmh}} = 0.104 \text{ in}$$

$$AG_{\text{bmh}} := AC_{\text{bm}} - \Delta L_{\text{bh}} + \Delta L_{\text{mpch}}$$

$$AG_{\text{bmh}} = 1.404 \text{ in}$$

3.U.5 Summary of Results

The previous results are summarized here.

MPC Shell-to-Overpack

$$RG_{moh} = 0.435 \text{ in}$$

$$AG_{moh} = 0.633 \text{ in}$$

Fuel Basket-to-MPC Shell

$$RG_{bmh} = 0.104 \text{ in}$$

$$AG_{bmh} = 1.404 \text{ in}$$

3.U.6 Nomenclature

a is the inner radius of the overpack

AC_{bm} is the initial fuel basket-to-MPC axial clearance.

AC_{mo} is the initial MPC-to-overpack axial clearance.

AG_{bmh} is the final fuel basket-to-MPC shell axial gap for the hot components.

AG_{moh} is the final MPC shell-to-overpack axial gap for the hot components.

b is the outer radius of the overpack.

L_{bas} is the axial length of the fuel basket.

L_{mpc} is the axial length of the MPC.

L_{ovp} is the axial length of the overpack.

r_1 (r_2, r_3, r_4) is mean radius of the overpack inner shell (shield shell, concrete, outer shell).

R_b is the outer radius of the fuel basket.

R_{mpc} is the mean radius of the MPC shell.

RC_{bm} is the initial fuel basket-to-MPC radial clearance.

RC_{mo} is the initial MPC shell-to-overpack radial clearance.

RG_{bmh} is the final fuel basket-to-MPC shell radial gap for the hot components.

RG_{moh} is the final MPC shell-to-overpack radial gap for the hot components.

t_1 (t_2, t_3, t_4) is the thickness of the overpack inner shell (shield shell, concrete, outer shell).

T_{bar} is the average temperature of the overpack cylinder.

α_1 ($\alpha_2, \alpha_3, \alpha_4$) is the coefficient of thermal expansion of the overpack inner shell (shield shell, concrete, outer shell).

α_{avg} is the average coefficient of thermal expansion of the overpack.

α_{bas} is the coefficient of thermal expansion of the overpack.

α_{mpc} is the coefficient of thermal expansion of the MPC.

ΔL_{bh} is the axial growth of the fuel basket for the hot components.

ΔL_{mpch} is the axial growth of the MPC for the hot components.
 ΔL_{ovph} is the axial growth of the overpack for the hot components.
 ΔR_{ah} is the radial growth of the overpack inner radius for the hot components.
 ΔR_{bh} is the radial growth of the fuel basket for the hot components.
 ΔR_{mpch} is the radial growth of the MPC shell for the hot components.
 ΔT_{1h} is the temperature change at the overpack inner shell for hot components.
 ΔT_{2h} is the temperature change at the overpack outer shell for hot components.
 ΔT_{3h} is the temperature change at the MPC shell mean radius for hot components.
 ΔT_{4h} is the temperature change at the MPC basket periphery for hot components.
 ΔT_{5h} is the temperature change at the MPC basket centerline for hot components.
 ΔT_{bas} is the fuel basket centerline-to-periphery temperature gradient.
 σ_{ca} is the circumferential stress at the overpack inner surface.
 σ_{cb} is the circumferential stress at the overpack outer surface.
 σ_r is the maximum radial stress of the overpack.
 σ_{z1} is the axial stress at the fuel basket centerline.
 σ_{z0} is the axial stress at the fuel basket periphery.

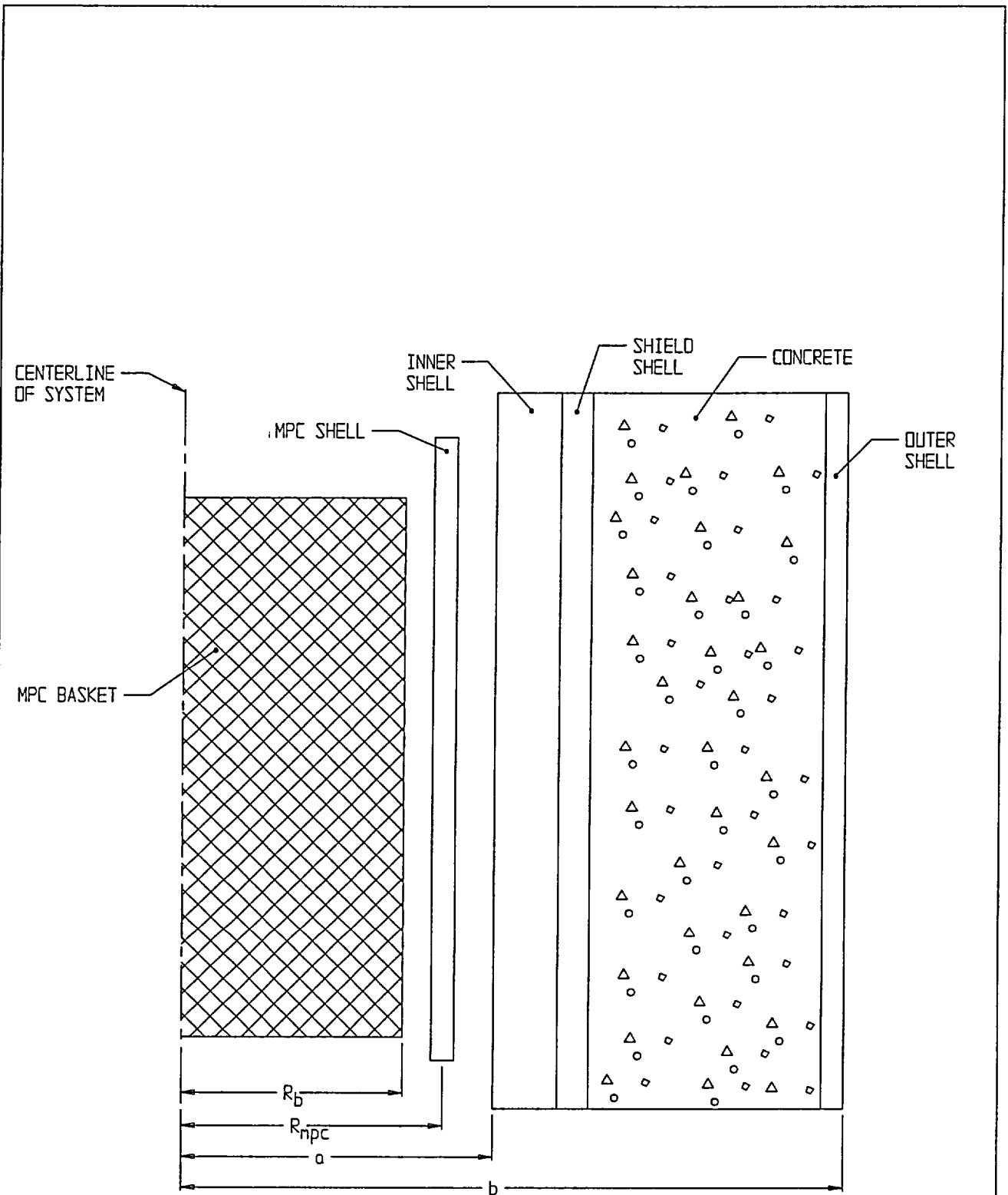


FIGURE 3.U.1; GEOMETRY OF SECTION FOR THERMAL EXPANSION CALCULATIONS

APPENDIX 3.V: HI-STORM 100 COMPONENT THERMAL EXPANSIONS; MPC-32

3.V.1 Scope

In this calculation, estimates of operating gaps, both radially and axially, are computed for the fuel basket-to-MPC shell, and for the MPC shell-to-overpack. This calculation is in support of the results presented in Section 3.4.4.2.

3.V.2 Methodology

Bounding temperatures are used to construct temperature distributions that will permit calculation of differential thermal expansions both radially and axially for the basket-to-MPC gaps, and for the MPC-to-overpack gaps. Reference temperatures are set at 70°F for all components. Temperature distributions are computed at the axial location of the HI-STORM 100 System where the temperatures are highest. A comprehensive nomenclature listing is provided in Section 3.V.6.

3.V.3 References

[3.V.1] Boley and Weiner, Theory of Thermal Stresses, John Wiley, 1960, Sec. 9.10, pp. 288-291.

[3.V.2] Burgreen, Elements of Thermal Stress Analysis, Arcturus Publishers, Cherry Hill NJ, 1988.

3.V.4 Calculations for Hot Components (Middle of System)

3.V.4.1 Input Data

Based on calculations in Chapter 4, the following temperatures are appropriate at the hottest axial location of the cask (see Figure 3.V.1 and Tables 4.4.26 and 4.4.36).

The temperature change at the overpack inner shell, $\Delta T_{1h} := 199 - 70$

The temperature change at the overpack outer shell, $\Delta T_{2h} := 145 - 70$

The temperature change at the mean radius of the MPC shell, $\Delta T_{3h} := 351 - 70$

The temperature change at the outside of the MPC basket, $\Delta T_{4h} := (496 - 70) \cdot 1.1$

The temperature change at the center of the basket (helium gas), $\Delta T_{5h} := 660 - 70$

Note that the outer basket temperature is conservatively amplified by 10% to insure a bounding parabolic distribution. This conservatism serves to maximize the growth of the basket.

The geometry of the components are as follows (referring to Figure 3.V.1)

The outer radius of the overpack, $b := 66.25$ in

The inner radius of the overpack, $a := 34.75$ in

The mean radius of the MPC shell, $R_{mpc} := \frac{68.375 \text{ in} - 0.5 \text{ in}}{2}$ $R_{mpc} = 33.938$ in

The initial MPC-to-overpack nominal radial clearance, $RC_{mo} := .5 \cdot (69.5 - 68.5) \text{ in}$
 $RC_{mo} = 0.5$ in

This initial radial clearance value, used to perform a radial growth check, is conservatively based on the channel radius and the maximum MPC diameter. For axial growth calculations for the MPC-to-overpack lid clearance, the axial length of the overpack is defined as the distance from the top of the pedestal platform to the bottom of the lid bottom plate, and the axial length of the MPC is defined as the overall MPC height.

The axial length of the overpack, $L_{ovp} := 191.5$ in

The axial length of the MPC, $L_{mpc} := 190.5$ in

The initial MPC-to-overpack nominal axial clearance, $AC_{mo} := L_{ovp} - L_{mpc}$

$$AC_{mo} = 1 \text{ in}$$

For growth calculations for the fuel basket-to-MPC shell clearances, the axial length of the basket is defined as the total length of the basket and the outer radius of the basket is defined as the mean radius of the MPC shell minus one-half of the shell thickness minus the initial basket-to-shell radial clearance.

The axial length of the basket, $L_{bas} := 176.5$ in

The initial basket-to-MPC lid nominal axial clearance, $AC_{bm} := 1.8125$ in

The initial basket-to-MPC shell nominal radial clearance, $RC_{bm} := 0.1875$ in

The outer radius of the basket, $R_b := R_{mpc} - \frac{0.5}{2} \text{ in} - RC_{bm}$ $R_b = 33.5$ in

The coefficients of thermal expansion used in the subsequent calculations are based on the mean temperatures of the MPC shell and the basket (conservatively estimated high).

The coefficient of thermal expansion for the MPC shell, $\alpha_{mpc} := 9.015 \cdot 10^{-6}$

The coefficient of thermal expansion for the basket, $\alpha_{bas} := 9.60 \cdot 10^{-6}$ 600 deg. F

3.V.4.2 Thermal Growth of the Overpack

Results for thermal expansion deformation and stress in the overpack are obtained here. The system is replaced by a equivalent uniform hollow cylinder with approximated average properties.

Based on the given inside and outside surface temperatures, the temperature solution in the cylinder is given in the form:

$$C_a + C_b \cdot \ln\left(\frac{r}{a}\right)$$

where

$$C_a := \Delta T_{1h} \quad C_a = 129$$

$$C_b := \frac{\Delta T_{2h} - \Delta T_{1h}}{\ln\left(\frac{b}{a}\right)} \quad C_b = -83\,688$$

Next, form the integral relationship:

$$\text{Int} := \int_a^b \left[C_a + C_b \cdot \ln\left(\frac{r}{a}\right) \right] \cdot r \, dr$$

The Mathcad program, which was used to create this appendix, is capable of evaluating the integral "Int" either numerically or symbolically. To demonstrate that the results are equivalent, the integral is evaluated both ways in order to qualify the accuracy of any additional integrations that are needed.

The result obtained through numerical integration, $\text{Int} = 1.533 \times 10^5 \text{ in}^2$

To perform a symbolic evaluation of the solution the integral "Ints" is defined. This integral is then evaluated using the Maple symbolic math engine built into the Mathcad program as:

$$\text{Int}_s := \int_a^b \left[C_a + C_b \cdot \ln\left(\frac{r}{a}\right) \right] \cdot r \, dr$$

$$\text{Int}_s := \frac{1}{2} \cdot C_b \cdot \ln\left(\frac{b}{a}\right) \cdot b^2 + \frac{1}{2} \cdot C_a \cdot b^2 - \frac{1}{4} \cdot C_b \cdot b^2 + \frac{1}{4} \cdot C_b \cdot a^2 - \frac{1}{2} \cdot C_a \cdot a^2$$

$$\text{Int}_s = 1.533 \times 10^5 \text{ in}^2$$

We note that the values of Int and Int_s are identical. The average temperature in the overpack cylinder (T_{bar}) is therefore determined as:

$$T_{\text{bar}} := \frac{2}{(b^2 - a^2)} \cdot \text{Int} \quad T_{\text{bar}} = 96.348$$

We estimate the average coefficient of thermal expansion for the overpack by weighting the volume of the various layers. A total of four layers are identified for this calculation. They are:

- 1) the inner shell
- 2) the shield shell
- 3) the radial shield
- 4) the outer shell

Note that the shield shell was removed from the HI-STORM 100 design as of 6:01. The replacement of the shield shell with concrete, however, has a negligible effect on the resultant coefficient of thermal expansion because (a) the difference in thermal expansion coefficients between concrete and carbon steel is small and (b) the shield shell accounts for a small percentage of the total overpack radial thickness.

Thermal properties are based on estimated temperatures in the component and coefficient of thermal expansion values taken from the tables in Chapter 3. The following averaging calculation involves the thicknesses (t) of the various components, and the estimated coefficients of thermal expansion at the components' mean radial positions. The results of the weighted average process yields an effective coefficient of linear thermal expansion for use in computing radial growth of a solid cylinder (the overpack).

The thicknesses of each component are defined as:

$$t_1 := 1.25 \cdot \text{in} \quad t_2 := 0.75 \cdot \text{in}$$

$$t_3 := 26.75 \cdot \text{in} \quad t_4 := 0.75 \cdot \text{in}$$

and the corresponding mean radii can therefore be defined as:

$$r_1 := a + .5 t_1 + 2 \text{ in}$$

$$r_2 := r_1 + .5 t_1 + 5 t_2$$

$$r_3 := r_2 + .5 t_2 + 5 t_3 \quad r_4 := r_3 + 5 t_3 + 5 t_4$$

To check the accuracy of these calculations, the outer radius of the overpack is calculated from r_4 and t_4 , and the result is compared with the previously defined value (b).

$$b_1 := r_4 + 0.5 \cdot t_4$$

$$b_1 = 66.25 \text{ in}$$

$$b = 66.25 \text{ in}$$

We note that the calculated value b_1 is identical to the previously defined value b . The coefficients of thermal expansion for each component, estimated based on the temperature gradient, are defined as:

$$\alpha_1 := 5.782 \cdot 10^{-6}$$

$$\alpha_2 := 5.782 \cdot 10^{-6}$$

$$\alpha_3 := 5.5 \cdot 10^{-6}$$

$$\alpha_4 := 5.638 \cdot 10^{-6}$$

Thus, the average coefficient of thermal expansion of the overpack is determined as:

$$\alpha_{avg} := \frac{r_1 \cdot t_1 \cdot \alpha_1 + r_2 \cdot t_2 \cdot \alpha_2 + r_3 \cdot t_3 \cdot \alpha_3 + r_4 \cdot t_4 \cdot \alpha_4}{\frac{a + b}{2} \cdot (t_1 + t_2 + t_3 + t_4)}$$

$$\alpha_{avg} = 5.628 \times 10^{-6}$$

Reference 3.V.1 gives an expression for the radial deformation due to thermal growth. At the inner radius of the overpack ($r = a$), the radial growth is determined as:

$$\Delta R_{ah} := \alpha_{avg} \cdot a \cdot T_{bar}$$

$$\Delta R_{ah} = 0.019 \text{ in}$$

Similarly, an overestimate of the axial growth of the overpack can be determined by applying the average temperature (T_{bar}) over the entire length of the overpack as:

$$\Delta L_{ovph} := L_{ovp} \cdot \alpha_{avg} \cdot T_{bar}$$

$$\Delta L_{ovph} = 0.104 \text{ in}$$

Estimates of the secondary thermal stresses that develop in the overpack due to the radial temperature variation are determined using a conservatively high value of E as based on the temperature of the steel. The circumferential stress at the inner and outer surfaces (σ_{ca} and σ_{cb} , respectively) are determined as:

The Young's Modulus of the material, $E := 28300000 \text{ psi}$

$$\sigma_{ca} := \alpha_{avg} \cdot \frac{E}{a^2} \cdot \left[2 \frac{a^2}{(b^2 - a^2)} \cdot \text{Int} - (C_a) \cdot a^2 \right]$$

$$\sigma_{ca} = -5200 \text{ psi}$$

$$\sigma_{cb} := \alpha_{avg} \cdot \frac{E}{b^2} \cdot \left[2 \frac{b^2}{(b^2 - a^2)} \cdot \text{Int} - \left[C_a + C_b \cdot \left(\ln \left(\frac{b}{a} \right) \right) \right] \cdot b^2 \right]$$

$$\sigma_{cb} = 3400 \text{ psi}$$

The radial stress due to the temperature gradient is zero at both the inner and outer surfaces of the overpack. The radius where a maximum radial stress is expected, and the corresponding radial stress, are determined by trial and error as:

$$N := 0.37$$

$$r := a(1 - N) + N \cdot b$$

$$r = 46.405 \text{ in}$$

$$\sigma_r := \alpha_{avg} \cdot \frac{E}{r^2} \cdot \left[\frac{r^2 - a^2}{2} \cdot T_{bar} - \int_a^r \left[C_a + C_b \cdot \left(\ln \left(\frac{y}{a} \right) \right) \right] \cdot y \, dy \right]$$

$$\sigma_r = -678201 \text{ psi}$$

The axial stress developed due to the temperature gradient is equal to the sum of the radial and tangential stresses at any radial location. (see eq. 9.10.7) of [3.V.1]. Therefore, the axial stresses are available from the above calculations. The stress intensities in the overpack due to the temperature distribution are below the Level A membrane stress.

3.V.4.3 Thermal Growth of the MPC Shell

The radial and axial growth of the MPC shell (ΔR_{mpch} and ΔL_{mpch} , respectively) are determined as:

$$\Delta R_{mpch} := \alpha_{mpc} \cdot R_{mpc} \cdot \Delta T_{3h} \qquad \Delta R_{mpch} = 0.086 \text{ in}$$

$$\Delta L_{mpch} := \alpha_{mpc} \cdot L_{mpc} \cdot \Delta T_{3h} \qquad \Delta L_{mpch} = 0.483 \text{ in}$$

3.V.4.4 Clearances Between the MPC Shell and Overpack

The final radial and axial MPC shell-to-overpack clearances (RG_{moh} and AG_{moh} , respectively) are determined as:

$$RG_{moh} := RC_{mo} + \Delta R_{ah} - \Delta R_{mpch}$$

$$RG_{moh} = 0.433 \text{ in}$$

$$AG_{moh} := AC_{mo} + \Delta L_{ovph} - \Delta L_{mpch}$$

$$AG_{moh} = 0.621 \text{ in}$$

Note that this axial clearance (AG_{moh}) is based on the temperature distribution at the middle of the system.

3.V.4.5 Thermal Growth of the MPC-32 Basket

Using formulas given in [3.V.2] for a solid body of revolution, and assuming a parabolic temperature distribution in the radial direction with the center and outer temperatures given previously, the following relationships can be developed for free thermal growth.

$$\text{Define } \Delta T_{bas} := \Delta T_{5h} - \Delta T_{4h} \quad \Delta T_{bas} = 121.4$$

$$\text{Then the mean temperature can be defined as } T_{bar} := \frac{2}{R_b^2} \int_0^{R_b} \left(\Delta T_{5h} - \Delta T_{bas} \cdot \frac{r^2}{R_b^2} \right) \cdot r \, dr$$

Using the Maple symbolic engine again, the closed form solution of the integral is:

$$T_{bar} := \frac{2}{R_b^2} \cdot \left(\frac{-1}{4} \cdot \Delta T_{bas} \cdot R_b^2 + \frac{1}{2} \cdot \Delta T_{5h} \cdot R_b^2 \right)$$

$$T_{bar} = 529.3$$

The corresponding radial growth at the periphery (ΔR_{bh}) is therefore determined as:

$$\Delta R_{bh} := \alpha_{bas} \cdot R_b \cdot T_{bar}$$

$$\Delta R_{bh} = 0.17 \text{ in}$$

and the corresponding axial growth (ΔL_{bas}) is determined from [3.V.2] as:

$$\Delta L_{bh} := \Delta R_{bh} \cdot \frac{L_{bas}}{R_b}$$

$$\Delta L_{bh} = 0.897 \text{ in}$$

Note that the coefficient of thermal expansion for the hottest basket temperature has been used, and the results are therefore conservative.

3.V.4.6 Clearances Between the Fuel Basket and MPC Shell

The final radial and axial fuel basket-to-MPC shell and lid clearances (RG_{bmh} and AG_{bmh} , respectively) are determined as:

$$RG_{bmh} := RC_{bm} - \Delta R_{bh} + \Delta R_{mpch}$$

$$RG_{bmh} = 0.103 \text{ in}$$

$$AG_{bmh} := AC_{bm} - \Delta L_{bh} + \Delta L_{mpch}$$

$$AG_{bmh} = 1.398 \text{ in}$$

3.V.5 Summary of Results

The previous results are summarized here.

MPC Shell-to-Overpack

$$RG_{moh} = 0.433 \text{ in}$$

$$AG_{moh} = 0.621 \text{ in}$$

Fuel Basket-to-MPC Shell

$$RG_{bmh} = 0.103 \text{ in}$$

$$AG_{bmh} = 1.398 \text{ in}$$

3.V.6 Nomenclature

a is the inner radius of the overpack

AC_{bm} is the initial fuel basket-to-MPC axial clearance.

AC_{mo} is the initial MPC-to-overpack axial clearance.

AG_{bmh} is the final fuel basket-to-MPC shell axial gap for the hot components.

AG_{moh} is the final MPC shell-to-overpack axial gap for the hot components.

b is the outer radius of the overpack.

L_{bas} is the axial length of the fuel basket.

L_{mpc} is the axial length of the MPC.

L_{ovp} is the axial length of the overpack.

r_1 (r_2, r_3, r_4) is mean radius of the overpack inner shell (shield shell, concrete, outer shell).

R_b is the outer radius of the fuel basket.

R_{mpc} is the mean radius of the MPC shell.

RC_{bm} is the initial fuel basket-to-MPC radial clearance.

RC_{mo} is the initial MPC shell-to-overpack radial clearance.

RG_{bmh} is the final fuel basket-to-MPC shell radial gap for the hot components.

RG_{moh} is the final MPC shell-to-overpack radial gap for the hot components.

t_1 (t_2, t_3, t_4) is the thickness of the overpack inner shell (shield shell, concrete, outer shell).

T_{bar} is the average temperature of the overpack cylinder.

α_1 ($\alpha_2, \alpha_3, \alpha_4$) is the coefficient of thermal expansion of the overpack inner shell (shield shell, concrete, outer shell).

α_{avg} is the average coefficient of thermal expansion of the overpack.

α_{bas} is the coefficient of thermal expansion of the overpack.

α_{mpc} is the coefficient of thermal expansion of the MPC.

ΔL_{bh} is the axial growth of the fuel basket for the hot components.

ΔL_{mpch} is the axial growth of the MPC for the hot components.
 ΔL_{ovph} is the axial growth of the overpack for the hot components.
 ΔR_{ah} is the radial growth of the overpack inner radius for the hot components.
 ΔR_{bh} is the radial growth of the fuel basket for the hot components.
 ΔR_{mpch} is the radial growth of the MPC shell for the hot components.
 ΔT_{1h} is the temperature change at the overpack inner shell for hot components.
 ΔT_{2h} is the temperature change at the overpack outer shell for hot components.
 ΔT_{3h} is the temperature change at the MPC shell mean radius for hot components.
 ΔT_{4h} is the temperature change at the MPC basket periphery for hot components.
 ΔT_{5h} is the temperature change at the MPC basket centerline for hot components.
 ΔT_{bas} is the fuel basket centerline-to-periphery temperature gradient.
 σ_{ca} is the circumferential stress at the overpack inner surface.
 σ_{cb} is the circumferential stress at the overpack outer surface.
 σ_r is the maximum radial stress of the overpack.
 σ_{z1} is the axial stress at the fuel basket centerline.
 σ_{z0} is the axial stress at the fuel basket periphery.

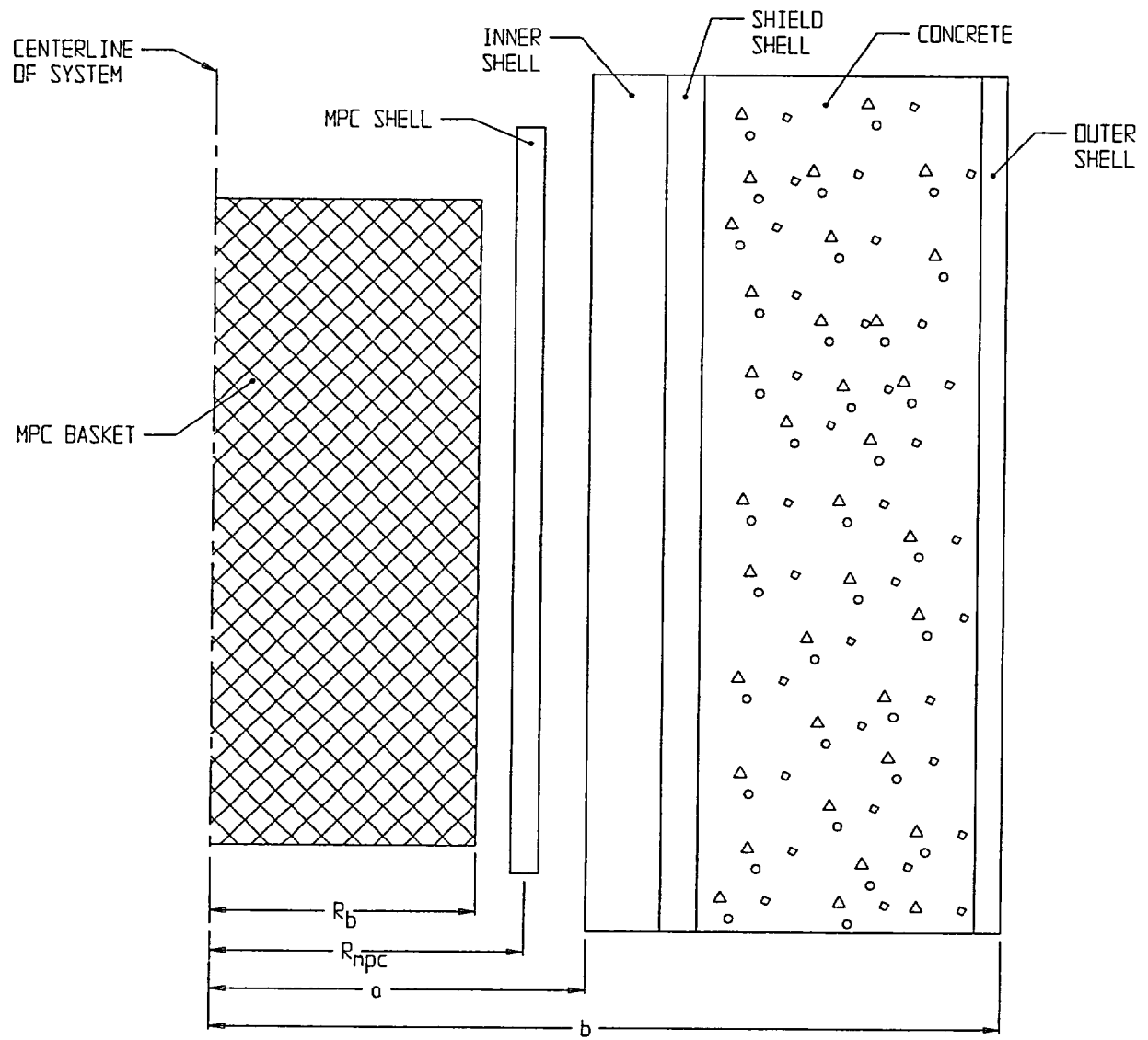


FIGURE 3.V.1; GEOMETRY OF SECTION FOR THERMAL EXPANSION CALCULATIONS

APPENDIX 3.W: HI-STORM 100 COMPONENT THERMAL EXPANSIONS; MPC-68

3.W.1 Scope

In this calculation, estimates of operating gaps, both radially and axially, are computed for the fuel basket-to-MPC shell, and for the MPC shell-to-overpack. This calculation is in support of the results presented in Section 3.4.4.2.

3.W.2 Methodology

Bounding temperatures are used to construct temperature distributions that will permit calculation of differential thermal expansions both radially and axially for the basket-to-MPC gaps, and for the MPC-to-overpack gaps. Reference temperatures are set at 70°F for all components. Temperature distributions are computed at the location of the HI-STORM 100 System where the temperatures are highest. A comprehensive nomenclature listing is provided in Section 3.W.6.

3.W.3 References

[3.W.1] Boley and Weiner, Theory of Thermal Stresses, John Wiley, 1960, Sec. 9.10, pp. 288-291.

[3.W.2] Burgreen, Elements of Thermal Stress Analysis, Arcturus Publishers, Cherry Hill NJ, 1988.

3.W.4 Calculations for Hot Components (Middle of System)

3.W.4.1 Input Data

Based on thermal calculations in Chapter 4, the following temperatures are appropriate at the hottest location of the cask (see Figure 3.W.1 and Tables 4.4.10 and 4.4.36).

The temperature change at the overpack inner shell, $\Delta T_{1h} := 199 - 70$ |

The temperature change at the overpack outer shell, $\Delta T_{2h} := 145 - 70$ |

The temperature change at the mean radius of the MPC shell, $\Delta T_{3h} := 347 - 70$ |

The temperature change at the outside of the MPC basket, $\Delta T_{4h} := (501 - 70) \cdot 1.1$ |

The temperature change at the center of the basket (helium gas), $\Delta T_{5h} := 720 - 70$ |

Note that the outer basket temperature is conservatively amplified by 10% to insure a bounding parabolic distribution. This conservatism serves to maximize the growth of the basket. The geometry of the components are as follows (referring to Figure 3.W.1)

The outer radius of the overpack, $b := 66.25 \text{ in}$

The inner radius of the overpack, $a := 34.75 \text{ in}$

The mean radius of the MPC shell, $R_{\text{mpc}} := \frac{68.375 \text{ in} - 0.5 \text{ in}}{2}$ $R_{\text{mpc}} = 33.938 \text{ in}$

The initial MPC-to-overpack nominal radial clearance, $RC_{\text{mo}} := .5 \cdot (69.5 - 68.5) \text{ in}$
 $RC_{\text{mo}} = 0.5 \text{ in}$

This initial radial clearance value, used to perform a radial growth check, is conservatively based on the channel radius (see Dwg. 1495, Sh. 5) and the maximum MPC diameter. For axial growth calculations for the MPC-to-overpack lid clearance, the axial length of the overpack is defined as the distance from the top of the pedestal platform to the bottom of the lid bottom plate, and the axial length of the MPC is defined as the overall MPC height.

The axial length of the overpack, $L_{\text{ovp}} := 191.5 \text{ in}$

The axial length of the MPC, $L_{\text{mpc}} := 190.5 \text{ in}$

The initial MPC-to-overpack nominal axial clearance, $AC_{\text{mo}} := L_{\text{ovp}} - L_{\text{mpc}}$

$$AC_{\text{mo}} = 1 \text{ in}$$

For growth calculations for the fuel basket-to-MPC shell clearances, the axial length of the basket is defined as the total length of the basket and the outer radius of the basket is defined as the mean radius of the MPC shell minus one-half of the shell thickness minus the initial basket-to-shell radial clearance.

The axial length of the basket, $L_{\text{bas}} := 176.5 \text{ in}$

The initial basket-to-MPC lid nominal axial clearance, $AC_{\text{bm}} := 1.8125 \text{ in}$

The initial basket-to-MPC shell nominal radial clearance, $RC_{\text{bm}} := 0.1875 \text{ in}$

The outer radius of the basket, $R_b := R_{\text{mpc}} - \frac{0.5}{2} \text{ in} - RC_{\text{bm}}$ $R_b = 33.5 \text{ in}$

The coefficients of thermal expansion used in the subsequent calculations are based on the mean temperatures of the MPC shell and the basket (conservatively estimated high).

The coefficient of thermal expansion for the MPC shell, $\alpha_{\text{mpc}} := 9.015 \cdot 10^{-6}$

The coefficient of thermal expansion for the basket, $\alpha_{\text{bas}} := 9.60 \cdot 10^{-6}$ 600 deg. F

3.W.4.2 Thermal Growth of the Overpack

Results for thermal expansion deformation and stress in the overpack are obtained here. The system is replaced by a equivalent uniform hollow cylinder with approximated average properties.

Based on the given inside and outside surface temperatures, the temperature solution in the cylinder is given in the form:

$$C_a + C_b \cdot \ln\left(\frac{r}{a}\right)$$

where

$$C_a := \Delta T_{1h} \quad C_a = 129$$

$$C_b := \frac{\Delta T_{2h} - \Delta T_{1h}}{\ln\left(\frac{b}{a}\right)} \quad C_b = -83.688$$

Next, form the integral relationship:

$$Int := \int_a^b \left[C_a + C_b \cdot \ln\left(\frac{r}{a}\right) \right] \cdot r \, dr$$

The Mathcad program, which was used to create this appendix, is capable of evaluating the integral "Int" either numerically or symbolically. To demonstrate that the results are equivalent, the integral is evaluated both ways in order to qualify the accuracy of any additional integrations that are needed.

The result obtained through numerical integration, $Int = 1.533 \times 10^5 \text{ in}^2$

To perform a symbolic evaluation of the solution the integral "Ints" is defined. This integral is then evaluated using the Maple symbolic math engine built into the Mathcad program as:

$$Int_s := \int_a^b \left[C_a + C_b \cdot \ln\left(\frac{r}{a}\right) \right] \cdot r \, dr$$

$$Int_s := \frac{1}{2} \cdot C_b \cdot \ln\left(\frac{b}{a}\right) \cdot b^2 + \frac{1}{2} \cdot C_a \cdot b^2 - \frac{1}{4} \cdot C_b \cdot b^2 + \frac{1}{4} \cdot C_b \cdot a^2 - \frac{1}{2} \cdot C_a \cdot a^2$$

$$Int_s = 1.533 \times 10^5 \text{ in}^2$$

We note that the values of Int and Ints are identical. The average temperature in the overpack cylinder (T_{bar}) is therefore determined as:

$$T_{\text{bar}} := \frac{2}{(b^2 - a^2)} \cdot \text{Int} \qquad T_{\text{bar}} = 96\,348$$

We estimate the average coefficient of thermal expansion for the overpack by weighting the volume of the various layers. A total of four layers are identified for this calculation. They are:

- 1) the inner shell
- 2) the shield shell
- 3) the radial shield
- 4) the outer shell

Note that the shield shell was removed from the HI-STORM 100 design as of 6/01. The replacement of the shield shell with concrete, however, has a negligible effect on the resultant coefficient of thermal expansion because (a) the difference in thermal expansion coefficients between concrete and carbon steel is small and (b) the shield shell accounts for a small percentage of the total overpack radial thickness.

Thermal properties are based on estimated temperatures in the component and coefficient of thermal expansion values taken from the tables in Chapter 3. The following averaging calculation involves the thicknesses (t) of the various components, and the estimated coefficients of thermal expansion at the components' mean radial positions. The results of the weighted average process yields an effective coefficient of linear thermal expansion for use in computing radial growth of a solid cylinder (the overpack).

The thicknesses of each component are defined as:

$$t_1 := 1.25 \cdot \text{in}$$

$$t_2 := 0.75 \cdot \text{in}$$

$$t_3 := 26.75 \cdot \text{in}$$

$$t_4 := 0.75 \cdot \text{in}$$

and the corresponding mean radii can therefore be defined as:

$$r_1 := a + .5 \cdot t_1 + 2.0 \text{ in} \qquad (\text{add the channel depth})$$

$$r_2 := r_1 + .5 \cdot t_1 + 5 \cdot t_2$$

$$r_3 := r_2 + .5 \cdot t_2 + .5 \cdot t_3$$

$$r_4 := r_3 + .5 \cdot t_3 + .5 \cdot t_4$$

To check the accuracy of these calculations, the outer radius of the overpack is calculated from r_4 and t_4 , and the result is compared with the previously defined value (b).

$$b_1 := r_4 + 0.5 \cdot t_4$$

$$b_1 = 66.25 \text{ in}$$

$$b = 66.25 \text{ in}$$

We note that the calculated value b_1 is identical to the previously defined value b . The coefficients of thermal expansion for each component, estimated based on the temperature gradient, are defined as:

$$\alpha_1 := 5.782 \cdot 10^{-6}$$

$$\alpha_2 := 5.782 \cdot 10^{-6}$$

$$\alpha_3 := 5.5 \cdot 10^{-6}$$

$$\alpha_4 := 5.638 \cdot 10^{-6}$$

Thus, the average coefficient of thermal expansion of the overpack is determined as:

$$\alpha_{\text{avg}} := \frac{r_1 \cdot t_1 \cdot \alpha_1 + r_2 \cdot t_2 \cdot \alpha_2 + r_3 \cdot t_3 \cdot \alpha_3 + r_4 \cdot t_4 \cdot \alpha_4}{\frac{a+b}{2} \cdot (t_1 + t_2 + t_3 + t_4)}$$

$$\alpha_{\text{avg}} = 5.628 \times 10^{-6}$$

Reference 3.W.1 gives an expression for the radial deformation due to thermal growth. At the inner radius of the overpack ($r = a$), the radial growth is determined as:

$$\Delta R_{\text{ah}} := \alpha_{\text{avg}} \cdot a \cdot T_{\text{bar}}$$

$$\Delta R_{\text{ah}} = 0.019 \text{ in}$$

Similarly, an overestimate of the axial growth of the overpack can be determined by applying the average temperature (T_{bar}) over the entire length of the overpack as:

$$\Delta L_{\text{ovph}} := L_{\text{ovp}} \cdot \alpha_{\text{avg}} \cdot T_{\text{bar}}$$

$$\Delta L_{\text{ovph}} = 0.104 \text{ in}$$

Estimates of the secondary thermal stresses that develop in the overpack due to the radial temperature variation are determined using a conservatively high value of E as based on the temperature of the steel. The circumferential stress at the inner and outer surfaces (σ_{ca} and σ_{cb} , respectively) are determined as:

The Young's Modulus of the material, $E := 28300000 \text{ psi}$

$$\sigma_{ca} := \alpha_{avg} \cdot \frac{E}{a^2} \cdot \left[2 \cdot \frac{a^2}{(b^2 - a^2)} \cdot \text{Int} - (C_a) \cdot a^2 \right]$$

$$\sigma_{ca} = -5200 \text{ psi}$$

$$\sigma_{cb} := \alpha_{avg} \cdot \frac{E}{b^2} \cdot \left[2 \cdot \frac{b^2}{(b^2 - a^2)} \cdot \text{Int} - \left[C_a + C_b \cdot \left(\ln \left(\frac{b}{a} \right) \right) \right] \cdot b^2 \right]$$

$$\sigma_{cb} = 3400 \text{ psi}$$

The radial stress due to the temperature gradient is zero at both the inner and outer surfaces of the overpack. The radius where a maximum radial stress is expected, and the corresponding radial stress, are determined by trial and error as:

$$N := 0.38$$

$$r := a \cdot (1 - N) + N \cdot b$$

$$r = 46.72 \text{ in}$$

$$\sigma_r = \alpha_{avg} \cdot \frac{E}{r^2} \cdot \left[\frac{r^2 - a^2}{2} \cdot T_{bar} - \int_a^r \left[C_a + C_b \cdot \left(\ln \left(\frac{y}{a} \right) \right) \right] \cdot y \, dy \right]$$

$$\sigma_r = -677.823 \text{ psi}$$

The axial stress developed due to the temperature gradient is equal to the sum of the radial and tangential stresses at any radial location. (see eq. 9.10.7) of [3.W.1]. Therefore, the axial stresses are available from the above calculations. The stress intensities in the overpack due to the temperature distribution are below the Level A membrane stress.

3.W.4.3 Thermal Growth of the MPC Shell

The radial and axial growth of the MPC shell (ΔR_{mpch} and ΔL_{mpch} , respectively) are determined as:

$$\Delta R_{mpch} := \alpha_{mpc} \cdot R_{mpc} \cdot \Delta T_{3h} \quad \Delta R_{mpch} = 0.085 \text{ in}$$

$$\Delta L_{mpch} := \alpha_{mpc} \cdot L_{mpc} \cdot \Delta T_{3h} \quad \Delta L_{mpch} = 0.476 \text{ in}$$

3.W.4.4 Clearances Between the MPC Shell and Overpack

The final radial and axial MPC shell-to-overpack clearances (RG_{moh} and AG_{moh} , respectively) are determined as:

$$RG_{moh} := RC_{mo} + \Delta R_{ah} - \Delta R_{mpch}$$

$$RG_{moh} = 0.434 \text{ in}$$

$$AG_{moh} := AC_{mo} + \Delta L_{ovph} - \Delta L_{mpch}$$

$$AG_{moh} = 0.628 \text{ in}$$

Note that this axial clearance (AG_{moh}) is based on the temperature distribution at the middle of the system.

3.W.4.5 Thermal Growth of the MPC-68 Basket

Using formulas given in [3.W.2] for a solid body of revolution, and assuming a parabolic temperature distribution in the radial direction with the center and outer temperatures given previously, the following relationships can be developed for free thermal growth.

$$\text{Define } \Delta T_{bas} := \Delta T_{5h} - \Delta T_{4h} \quad \Delta T_{bas} = 175.9$$

$$\text{Then the mean temperature can be defined as } T_{bar} := \frac{2}{R_b^2} \int_0^{R_b} \left(\Delta T_{5h} - \Delta T_{bas} \cdot \frac{r^2}{R_b^2} \right) \cdot r \, dr$$

Using the Maple symbolic engine again, the closed form solution of the integral is:

$$T_{\text{bar}} := \frac{2}{R_b^2} \left(\frac{-1}{4} \cdot \Delta T_{\text{bas}} \cdot R_b^2 + \frac{1}{2} \cdot \Delta T_{5h} \cdot R_b^2 \right)$$

$$T_{\text{bar}} = 562.05$$

The corresponding radial growth at the periphery (ΔR_{bh}) is therefore determined as:

$$\Delta R_{\text{bh}} := \alpha_{\text{bas}} \cdot R_b \cdot T_{\text{bar}} \qquad \Delta R_{\text{bh}} = 0.181 \text{ in}$$

and the corresponding axial growth (ΔL_{bas}) is determined from [3.W.2] as:

$$\Delta L_{\text{bh}} := \Delta R_{\text{bh}} \cdot \frac{L_{\text{bas}}}{R_b}$$

$$\Delta L_{\text{bh}} = 0.952 \text{ in}$$

Note that the coefficient of thermal expansion for the hottest basket temperature has been used, and the results are therefore conservative.

3.W.4.6 Clearances Between the Fuel Basket and MPC Shell

The final radial and axial fuel basket-to-MPC shell and lid clearances (RG_{bmh} and AG_{bmh} , respectively) are determined as:

$$RG_{\text{bmh}} := RC_{\text{bm}} - \Delta R_{\text{bh}} + \Delta R_{\text{mpch}}$$

$$RG_{\text{bmh}} = 0.091 \text{ in}$$

$$AG_{\text{bmh}} := AC_{\text{bm}} - \Delta L_{\text{bh}} + \Delta L_{\text{mpch}}$$

$$AG_{\text{bmh}} = 1.336 \text{ in}$$

3.W.5 Summary of Results

The previous results are summarized here.

MPC Shell-to-Overpack

$$RG_{moh} = 0.434 \text{ in}$$

$$AG_{moh} = 0.628 \text{ in}$$

Fuel Basket-to-MPC Shell

$$RG_{bmh} = 0.091 \text{ in}$$

$$AG_{bmh} = 1.336 \text{ in}$$

3.W.6 Nomenclature

a is the inner radius of the overpack

AC_{bm} is the initial fuel basket-to-MPC axial clearance.

AC_{mo} is the initial MPC-to-overpack axial clearance.

AG_{bmh} is the final fuel basket-to-MPC shell axial gap for the hot components.

AG_{moh} is the final MPC shell-to-overpack axial gap for the hot components.

b is the outer radius of the overpack.

L_{bas} is the axial length of the fuel basket.

L_{mpc} is the axial length of the MPC.

L_{ovp} is the axial length of the overpack.

r_1 (r_2, r_3, r_4) is mean radius of the overpack inner shell (shield shell, concrete, outer shell).

R_b is the outer radius of the fuel basket.

R_{mpc} is the mean radius of the MPC shell.

RC_{bm} is the initial fuel basket-to-MPC radial clearance.

RC_{mo} is the initial MPC shell-to-overpack radial clearance.

RG_{bmh} is the final fuel basket-to-MPC shell radial gap for the hot components.

RG_{moh} is the final MPC shell-to-overpack radial gap for the hot components.

t_1 (t_2, t_3, t_4) is the thickness of the overpack inner shell (shield shell, concrete, outer shell).

T_{bar} is the average temperature of the overpack cylinder.

α_1 ($\alpha_2, \alpha_3, \alpha_4$) is the coefficient of thermal expansion of the overpack inner shell (shield shell, concrete, outer shell).

α_{avg} is the average coefficient of thermal expansion of the overpack.

α_{bas} is the coefficient of thermal expansion of the overpack.

α_{mpc} is the coefficient of thermal expansion of the MPC.

ΔL_{bh} is the axial growth of the fuel basket for the hot components.

ΔL_{mpch} is the axial growth of the MPC for the hot components.
 ΔL_{ovph} is the axial growth of the overpack for the hot components.
 ΔR_{ah} is the radial growth of the overpack inner radius for the hot components.
 ΔR_{bh} is the radial growth of the fuel basket for the hot components.
 ΔR_{mpch} is the radial growth of the MPC shell for the hot components.
 ΔT_{1h} is the temperature change at the overpack inner shell for hot components.
 ΔT_{2h} is the temperature change at the overpack outer shell for hot components.
 ΔT_{3h} is the temperature change at the MPC shell mean radius for hot components.
 ΔT_{4h} is the temperature change at the MPC basket periphery for hot components.
 ΔT_{5h} is the temperature change at the MPC basket centerline for hot components.
 ΔT_{bas} is the fuel basket centerline-to-periphery temperature gradient.
 σ_{ca} is the circumferential stress at the overpack inner surface.
 σ_{cb} is the circumferential stress at the overpack outer surface.
 σ_r is the maximum radial stress of the overpack.
 σ_{z1} is the axial stress at the fuel basket centerline.
 σ_{z0} is the axial stress at the fuel basket periphery.

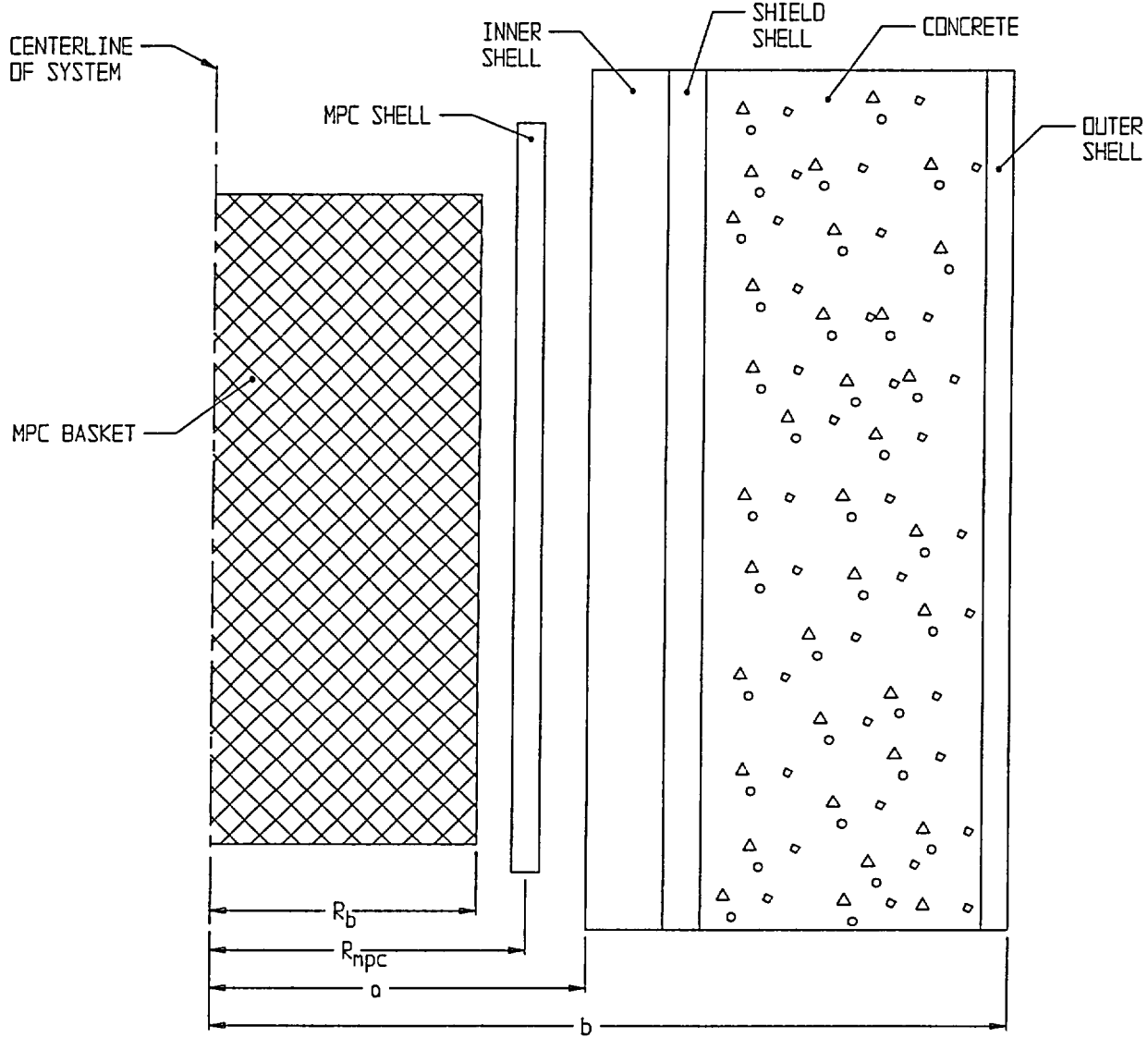


FIGURE 3.W.1; GEOMETRY OF SECTION FOR THERMAL EXPANSION CALCULATIONS

APPENDIX 3.X CALCULATION OF DYNAMIC LOAD FACTORS

3.X.1 Introduction

In Appendix 3.A, the rigid body deceleration sustained by a loaded HI-STORM 100 system under postulated drop events has been calculated. The deceleration profile encompassed by the first half cycle is found to be approximated by a triangular half-wave. It is recognized that the local structural flexibility of the structural members within the cask would modify the net equivalent inertia load for which the member is subjected.

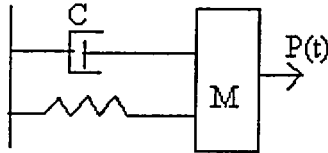
In classical elastic stress analysis, a dynamic load factor (DLF) is determined to reflect the local dynamic effects due to local flexibilities. The DLF is a function of the frequency content of the component being analyzed, the postulated level of structural damping, and the shape and duration of the input load pulse. For most structural elements, it is adequate to compute the fundamental frequency of the element and utilize the classical DLF charts to establish the DLF for the specified impulse. However, in more complicated situations, it is necessary to determine the DLF using a direct numerical formulation. For example, the DLF of the cask lid under a lateral excitation can be readily established from a structural dynamics textbook chart for a wide variety of pulse shapes. On the other hand, the case of lateral excitation of a fuel basket, which involves simultaneous deceleration of the self mass of the panel along with a much heavier fuel assembly mass, requires a direct time integration solution. The fuel assembly is modeled as a lumped compliant mass "riding" the fuel basket panel mass during the impulsive deceleration event. Thus, the fuel basket DLF problem is modeled as a two-degree of freedom system with the basket panel represented by a single degree of freedom mass-spring-damper system (consistent with its fundamental mode) with the added spent nuclear fuel (SNF) mass appended to it, but not permanently affixed. The SNF should be assumed to be plastically connected; i.e., the coefficient of restitution set equal to zero to simulate the absence of springback and to render the dynamic analysis consistent with the "lumped uniform load" modeling of the SNF effect in the static stress analysis of the fuel basket.

Therefore, to cover all structural cases within the cask, both a single-degree of freedom spring-mass-damper system and a multi-mass system with contacting compliant surface, are subject to a pulse load of duration and shape consistent with the dynamic drop analyses to determine the appropriate DLF.

The DLF is defined as the ratio of the peak dynamic displacement of the structural mass when subject to a time dependent pulse force with peak amplitude F , to the corresponding static displacement of the structural mass when subject to the constant force amplitude F . Since the displacement in the dynamic models is related to the elastic internal energy imparted to the component, the calculation of the DLF in this manner properly reflects any increase in the stress levels in a corresponding static analysis.

3 X.2 Analysis Models

3.X.2.1 Components Modeled by Single Degree of Freedom Systems



The following items are defined:

c = damping coefficient

M = mass contributing to dynamic motion

k = spring constant

$P(t)$ = pulse loading with peak value F

$x(t)$ = displacement of mass M

If the pulse force is defined as $P(t) = F * f(t)$ where the maximum value of $f(t)$ is 1.0, then F is the peak force magnitude and the static solution x_s may be defined as

$$x_s = F/k$$

For the determination of the DLF for the cask system, it is appropriate to use a half triangular wave as a pulse, with duration of the pulse equal to t_p . The dynamic load factor (DLF) is the maximum value of the ratio x/x_s that occurs for a total event time $\gg t_p$.

The input triangular pulse shape is defined in Figure 3.X.1.

F is the peak value of the pulse shape and t_p is the duration of the half-pulse. The solution for the single degree of freedom undamped system is given in [3 X.3,(Section 4, p125,128)]. The results are reproduced in Figure 3.X.2. The graph plots the ratio of the maximum dynamic response x to the static response F/k (i.e., the DLF) versus the ratio of the triangular pulse duration divided by the period associated with the natural frequency of the single degree of freedom system.

3.X.2.2 Components Modeled by Multiple Degree of Freedom Systems

The MPC fuel basket has been stress analyzed using finite element analysis methods assuming that the applied load is a design basis constant deceleration. The spent fuel mass, which is heavier than a fuel basket panel, is conservatively assumed to be a very compliant component with no structural stiffness and to transfer load to the panel element as a uniform pressure acting on the panel surface. In the actual dynamic environment, the fuel assembly mass is confined, during a drop event, by the surrounding walls of the basket, but is not physically attached to the fuel basket. To derive an appropriate dynamic load factor, the configuration consisting of the confining panels and the fuel mass must be modeled and the assemblage subjected to the appropriate triangular pulse shape and time duration. The peak displacement response of the panel mass is then compared to the static response under a static deceleration having the same peak to define the appropriate DLF. The specific configuration analyzed for determination of dynamic load factors is shown in Figure 3.X.3. The solution to this problem is obtained using the commercial computer code "Working Model" which has been subject to independent Quality Assurance verification and validation at Holtec International. Working Model is ideally suited to the solution of dynamics problems involving multiple masses in contact with each other and is also utilized in the HI-STAR 100 Part 71 SAR submittal for a transport license to analyze impact limiter performance under hypothetical accident conditions. Specific results are reported in a subsequent section of this appendix.

In Figure 3.X.3, the SNF assembly is confined by the basket wall panels; the inertia load resulting from the deceleration pulse is applied to the SNF and to the panels. The structural configuration is simulated by a mass-spring system representing the lower supporting panel, by a compliant lumped mass representing the SNF assembly, and by a second mass-spring system representing the confining panel above the SNF mass. The two linear springs represent the structural flexibility of the basket panels. The applied time varying inertia force which is applied to each of the masses is equal to the respective mass multiplied by a triangular shaped pulse with peak value equal to the specified drop deceleration. The compliant spent fuel assembly contact is simulated by using a coefficient of restitution value near zero which is consistent with the assumption in the static stress analysis that the fuel loading is a uniform load over the panel surface because the SNF assembly follows the panel deformation.

In subsequent sections, an evaluation of potential DLF magnitudes is carried out for representative components of HI-STORM. While a number of cask components are examined to determine fundamental frequency, DLF's are computed only for those components most affected.

3.X.3 References

[3.X.1] H.A. Rothbart, Mechanical Design and Systems Handbook, 2nd Edition, McGraw Hill, 1985.

[3.X.2] Working Model 3.0, Knowledge Revolution, San Mateo, CA., 1995.

[3.X.3] W.T. Thomson, Theory of Vibration With Applications, 2nd Edition, Prentice Hall, 1981, Section 7.4, p. 220.

3.X.4 Dynamic Characteristics of an MPC Fuel Basket Panel Subject to Lateral Drops-Preliminary Calculations

The most significant loading level applied to a HI-STAR 100 component occurs during drop conditions. In particular, the fuel basket, under side drop or tipover, may have individual panels subjected to high levels of lateral load. Since the stress analyses of the basket is based on static methods, the results must be amplified by a DLF prior to performing a structural integrity evaluation involving comparison against specified stress or stress intensity levels. As described previously, the DLF depends on the product of component natural frequency and impulse time duration. Appendix 3.A presents the analysis of the postulated drop events appropriate for a 10CFR72 submittal and computes impulse durations. Here we compute appropriate dynamic load factors using the multi-mass model described previously, with a range of pulse durations. Calculations are made and results obtained for both PWR and BWR fuel baskets.

For the dynamic simulation, the panel flexibilities, the panel fundamental frequency (or period), and the effective panel mass participating in the dynamics of the configuration must be established. The panel section perpendicular to the applied deceleration pulse is modeled by a beam clamped at both ends (to the adjacent perpendicular panel). Figure 3.X.4 defines the configuration and the variables.

From Table 7.1 of [3.X.1], the spring constant of a clamped-clamped beam is given as

$$K := 384 \cdot \frac{E \cdot I}{L^3}$$

Input data for the Holtec MPC-24 basket is (L is the panel width, t is the panel metal thickness, and b is approximately equal to the total length of the panel along the axis of the cask). For conservatism, we use the pitch as the panel width to obtain a lower natural frequency.

$$L := 10.777 \cdot \text{in} \quad t := \frac{10}{32} \cdot \text{in} \quad b := 176.5 \cdot \text{in}$$

At 725 deg. F the Young's Modulus is $E := 24600000 \cdot \text{psi}$ (Table 3.3.1)

The actual weight of the modeled stainless steel panel is

$$W_{\text{actual}} := 0.29 \cdot \frac{\text{lb}}{\text{in}^3} \cdot b \cdot L \cdot t \quad W_{\text{actual}} = 172.3815 \text{ lbf} \quad \text{Overestimated because of density.}$$

Compute the moment of inertia "I" and the cross section area "A" perpendicular to the bending axis.

$$I := b \cdot \frac{t^3}{12} \quad A := b \cdot t$$

Therefore, the spring constant K is given, for the PWR panel, as (use the entire length "b")

$$K := 384 \cdot \frac{E \cdot I}{L^3} \quad K = 3.3876 \times 10^6 \frac{\text{lb}}{\text{in}}$$

Compute the natural frequency of the panel considered as a clamped-clamped beam.

The natural frequency is computed from a formula and tables given in [3.X.1] (Chap. 5 and Tables 5.8(c) and 5.10). The nomenclature that used in the reference.

$$K_m := 0.9 \quad C_n := 71.95$$

Therefore the lowest natural frequency of the panel is

$$f_n := C_n \cdot \frac{\sqrt{\frac{I}{A}}}{L^2} \cdot 10^4 \cdot K_m \cdot \frac{\text{in}}{\text{sec}} \quad f_n = 502.964 \text{ sec}^{-1} \quad \tau_{pwr} := \frac{1}{f_n}$$

$$\omega_n = 2 \cdot \pi \cdot f_n \quad \omega_n = 3.1602 \times 10^3 \text{ sec}^{-1} \quad \tau_{pwr} = 1.9882 \times 10^{-3} \text{ sec}$$

The effective panel mass participating in the dynamic motion is computed as

$$m_e := \frac{K}{\omega_n^2}$$

The effective participating weight of the panel is

$$W_{PWR} := m_e \cdot g \quad W_{PWR} = 130.9603 \text{ lbf}$$

which is, as expected, less than the actual weight.

The calculations are now repeated for a BWR panel

$$L := 6.24 \cdot \text{in} \quad t := \frac{8}{32} \cdot \text{in} \quad b := 176 \cdot \text{in}$$

The actual weight of the stainless steel panel is

$$W_{\text{actual}} := 0.29 \cdot \frac{\text{lbf}}{\text{in}^3} \cdot b \cdot L \cdot t \quad W_{\text{actual}} = 79.6224 \text{ lbf}$$

Compute the moment of inertia "I" and the cross section area "A" perpendicular to the bending axis.

$$I := b \cdot \frac{t^3}{12} \quad A := b \cdot t$$

Therefore, the spring constant K is given as

$$K := 384 \cdot \frac{E \cdot I}{L^3} \quad K = 8.9097 \times 10^6 \frac{\text{lbf}}{\text{in}}$$

Compute natural frequency of the panel considered as a clamped-clamped beam

$$K_m := 0.9 \quad C_n := 71.95$$

$$f_n := C_n \cdot \frac{\sqrt{\frac{I}{A}}}{L^2} \cdot 10^4 \cdot K_m \cdot \frac{\text{in}}{\text{sec}} \quad f_n = 1.2002 \times 10^3 \text{ sec}^{-1}$$

$$\tau_{\text{bwr}} := \frac{1}{f_n} \quad \tau_{\text{bwr}} = 8.3319 \times 10^{-4} \text{ sec}$$

$$\omega_n := 2 \cdot \pi \cdot f_n \quad \omega_n = 7.5411 \times 10^3 \text{ sec}^{-1}$$

The effective mass participating in the dynamic motion is computed as

$$m_e := \frac{K}{\omega_n^2}$$

The effective participating weight of the panel is

$$W_{\text{BWR}} := m_e \cdot g \quad W_{\text{BWR}} = 60.4901 \text{ lbf}$$

3.X.5 Analysis for Dynamic Load Factors for the HI-STORM Fuel Basket Subject to Handling Accidents Resulting in a Lateral Deceleration Pulse - Multi-Degree of Freedom System

The data developed in Section 3.X.4 is used as input data in Working Model to determine dynamic amplification factors. The description of the model is provided in Section 3.X.2.2. Fuel weights used in the multi-mass model are the design basis fuel weights (Table 2.1.6). To determine the DLF, the peak deflection of the panel needs to be established. The DLF is obtained as the maximum ratio of the spring force resisting the dynamic deceleration load, divided by the static spring force obtained if the peak value of the deceleration was applied statically. In this simulation, only drop orientations causing lateral panel bending are significant. Results are computed here for a load of 50g's and pulse time duration of 10 milliseconds. This set of inputs is representative of the results from Appendix 3.A

$$G_{10} := 50$$

The quasi-static force in the spring induced by dead load plus drop inertia load is easily computed for the two basket types as

$$\text{Force_PWR}_{10} := (1680 \cdot \text{lbf} + W_{\text{PWR}}) \cdot (G_{10} + 1) \qquad \text{Force_PWR}_{10} = 9.2359 \times 10^4 \text{ lbf}$$

$$\text{Force_BWR}_{10} := (700 \cdot \text{lbf} + W_{\text{BWR}}) \cdot (G_{10} + 1) \qquad \text{Force_BWR}_{10} = 3.8785 \times 10^4 \text{ lbf}$$

The Working Model analyses are performed for both types of fuel baskets with deceleration pulses of triangular shape and with the appropriate time duration. In the simulations, the coefficient of restitution between the SNF mass and the panel masses is set to 0.0 to be consistent with a fully compliant case. As is noted above, the use of a zero coefficient of restitution is consistent with the completely compliant SNF mass assumption which permeates all of the basket stress analyses. Figures 3.X.4-3.X.5 provide the time history of the force in the loaded lower panel spring for the PWR, BWR baskets, respectively. For each case, the DLF is obtained by dividing the peak dynamic spring force by the static spring forces computed above (note that since the spring forces are linear functions of the panel central deflection, the DLF is directly calculated from the spring force results). The peak forces are

$$F_{\text{peak_PWR}} := 99500 \cdot \text{lbf}$$

$$F_{\text{peak_BWR}} := 41130 \cdot \text{lbf}$$

Therefore, the DLF's are

$$\text{DLF}_{\text{PWR}} := \frac{F_{\text{peak_PWR}}}{\text{Force_PWR}_{10}}$$

$$\text{DLF}_{\text{PWR}} = 1.0773$$

$$\text{DLF}_{\text{BWR}} := \frac{F_{\text{peak_BWR}}}{\text{Force_BWR}_{10}}$$

$$\text{DLF}_{\text{BWR}} = 1.0605$$

3 X.6 Overpack Lid Top Plate Considered as a Simply Supported Circular Plate

3.X 6.1 Input Data

SA516 Young's Modulus at 350°F (Table 3.3.2), $E := 28 \cdot 10^6 \cdot \text{psi}$

SA516 Poisson's ratio (Section 3.3), $\nu := .3$

Metal weight density (Section 3.3), $\gamma := 0.29 \cdot \frac{\text{lbf}}{\text{in}^3}$

The following dimensions are taken from Holtec drawing no. 1495. The total weight for the lower of the two plates, plus the lid shield, the lid shell and the lid bottom plate. From Appendix 3.K

Weight := 12336 lbf

In the subsequent analysis, we use a bounding weight of 13500 lbf.

Weight := 13500 · lbf

$R := \frac{75}{2} \cdot \text{in}$ Support radius (assumed larger than inner shell radius)

$h := 2 \cdot \text{in}$ Lid thickness Use only one of the lids

3 X.6.2 Calculations

$$D := \frac{E \cdot h^3}{12 \cdot (1 - \nu^2)}$$

$$\gamma := \frac{\text{Weight}}{h \cdot \pi \cdot R^2} \quad \gamma = 1.528 \frac{\text{lbf}}{\text{in}^3} \quad \text{Effective density}$$

The effective density is higher than steel because all of the weight is placed inside the support circle.

$$f_i := \frac{5.251}{2 \cdot \pi \cdot R^2} \cdot \sqrt{g \cdot \frac{D}{\gamma \cdot h}} \quad f_i = 30 \, 2549 \text{ Hz} \quad [3 \text{ X.1}]$$

3 X.7 Overpack Lid Bottom Plate (supporting concrete) Considered as a Clamped Circular Plate

3 X.7 1 Input Data

SA516 Young's Modulus at 350°F (Table 3 3.2), $E := 28.0 \cdot 10^6 \text{ psi}$

SA516 Poisson's ratio (Section 3.3),

$$\nu := .3$$

Metal weight density (Section 3.3),

$$\gamma := 0.29 \cdot \frac{\text{lbf}}{\text{in}^3}$$

The following dimensions are taken from Holtec drawing no. 1495.

$h := 1.25 \cdot \text{in}$ Lid thickness

$R := \frac{68.375}{2} \cdot \text{in}$ Support radius

3.X.7.2 Calculations

$$D := \frac{E \cdot h^3}{12 \cdot (1 - \nu^2)}$$

$$f_{lb} := \frac{10.21}{2 \cdot \pi \cdot R^2} \cdot \sqrt{g \cdot \frac{D}{\gamma \cdot h}} \qquad f_{lb} = 101.5391 \text{ Hz} \qquad [3.X.1]$$

3.X.8 Dynamic Load Factor Upper Bound Estimates for Storage Loading Events

3.X.8.1 End Drop

Use Lower bound weight estimate and upper bound pad stiffness. From results in Appendix 3.A, the duration of the impact in an end drop event is

$$t_{pe} := .003 \cdot \text{sec}$$

The DLF for the Overpack Lid Top Plate is based on a bottom end drop and the single degree of freedom model employed. The ratio of the period of the pulse to the fundamental period is

$$f_1 \cdot t_{pe} = 0.091$$

Figure 3.X.2 demonstrates that there is no dynamic amplification at this ratio (DLF < 1). Conservatively, we use the DLF as:

$$\text{DLF} := 1.00$$

The DLF for the Overpack Lid Bottom Plate is based on a bottom end drop

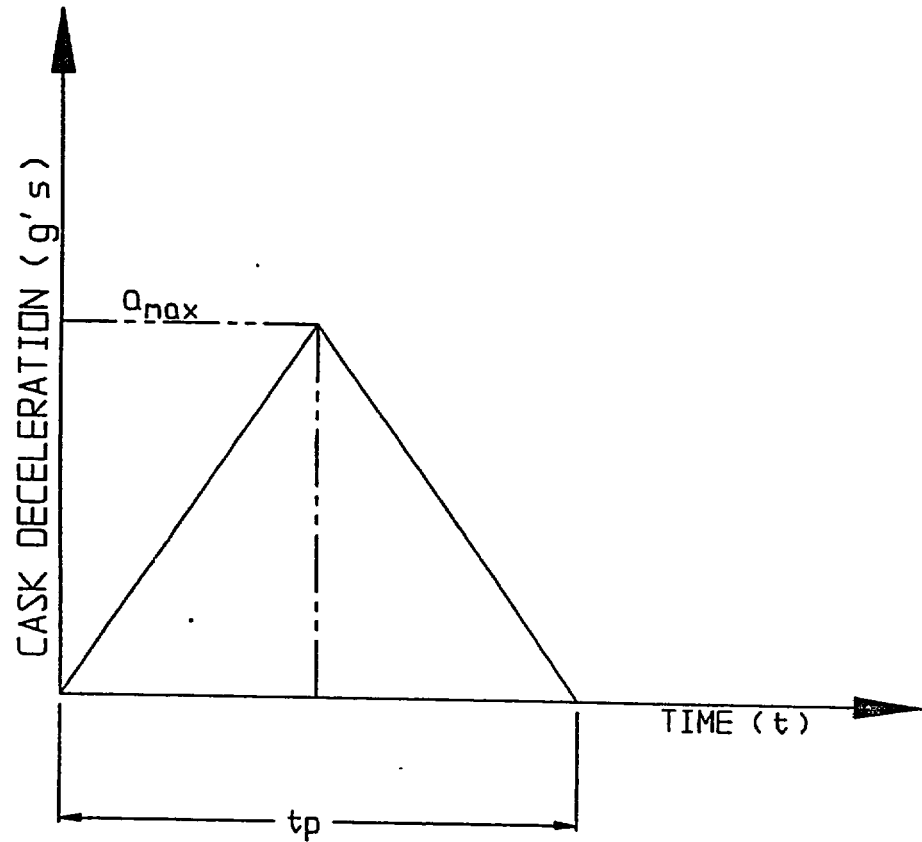
$$f_{lb} \cdot t_{pe} = 0.3$$

From Figure 3 X 2, we use a dynamic amplification factor that is conservatively chosen

$$\text{DLF} := 1.06$$

3 X.9 Conclusions

Dynamic Load Factor Equations have been obtained in this appendix. All static stress calculations use these dynamic load amplifiers to evaluate the adequacy of final safety factors.



a_{max} :	PEAK g LEVEL (FILTERED DATA)
t_p :	PULSE DURATION (sec)

FIGURE 3.X.1 : TRIANGULAR DECELERATION PULSE SHAPE

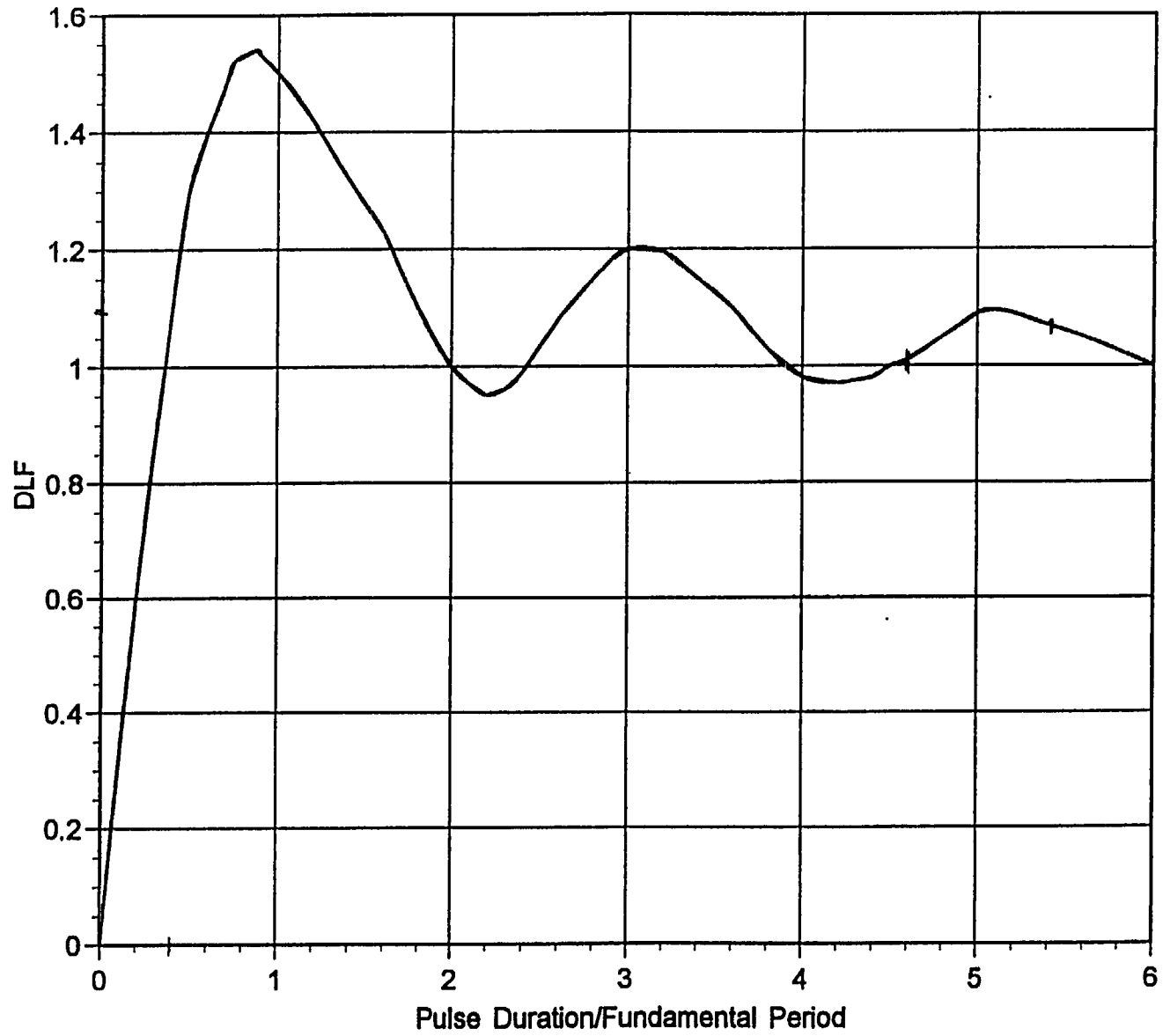


FIGURE 3.X.2 - Dynamic Load Factor for Single Degree of Freedom System - Triangular Pulse Shape, No Damping

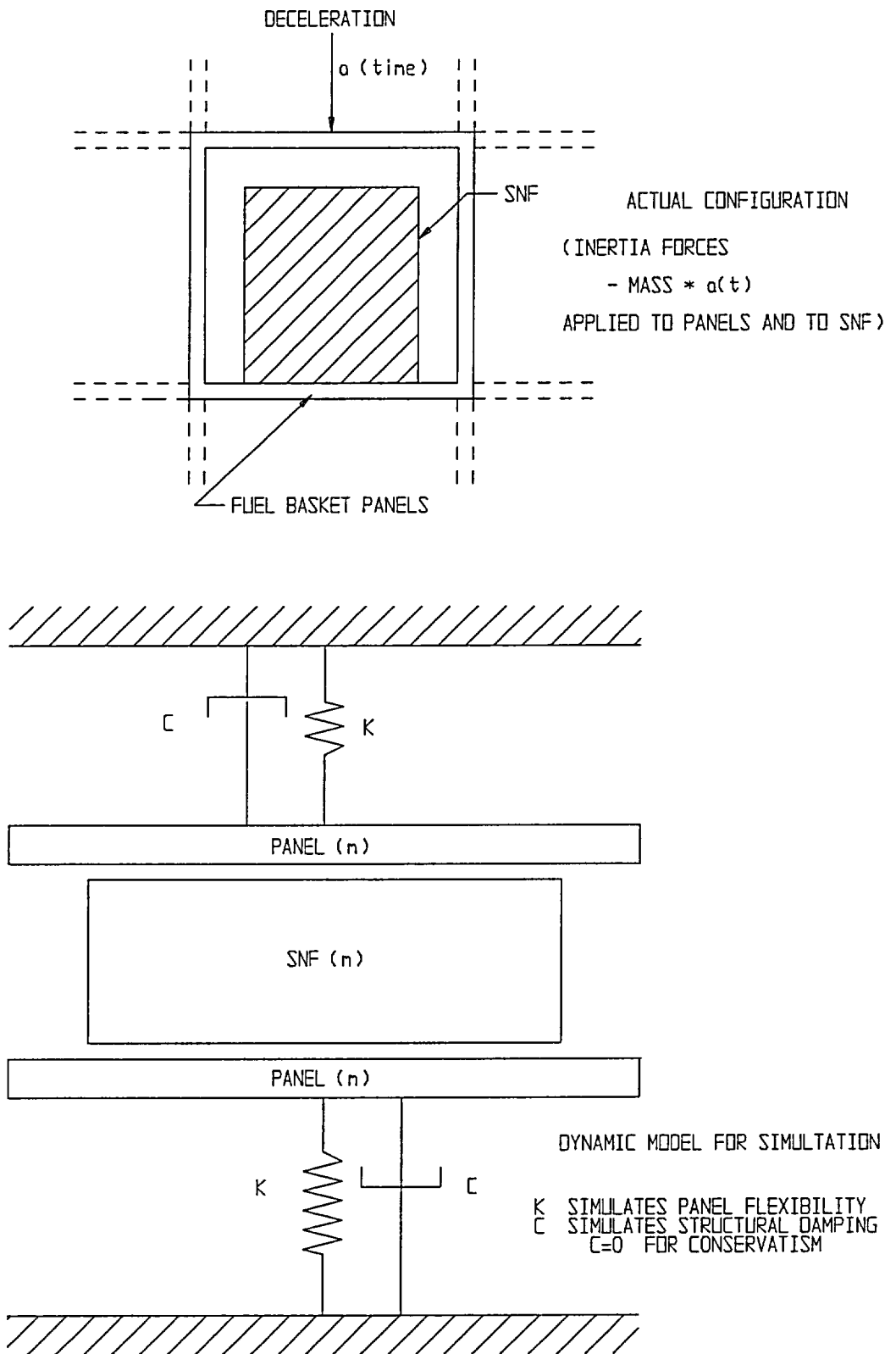
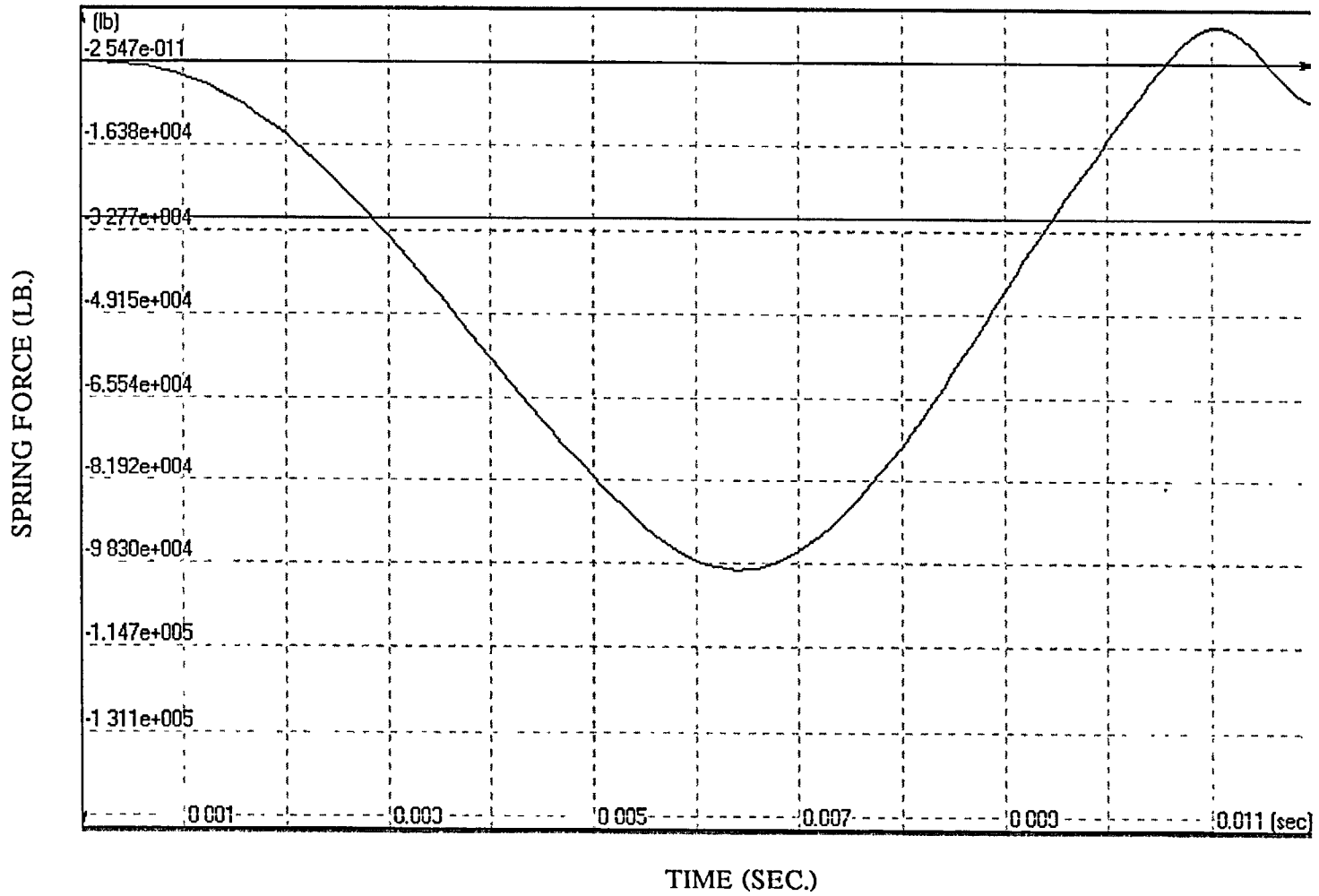
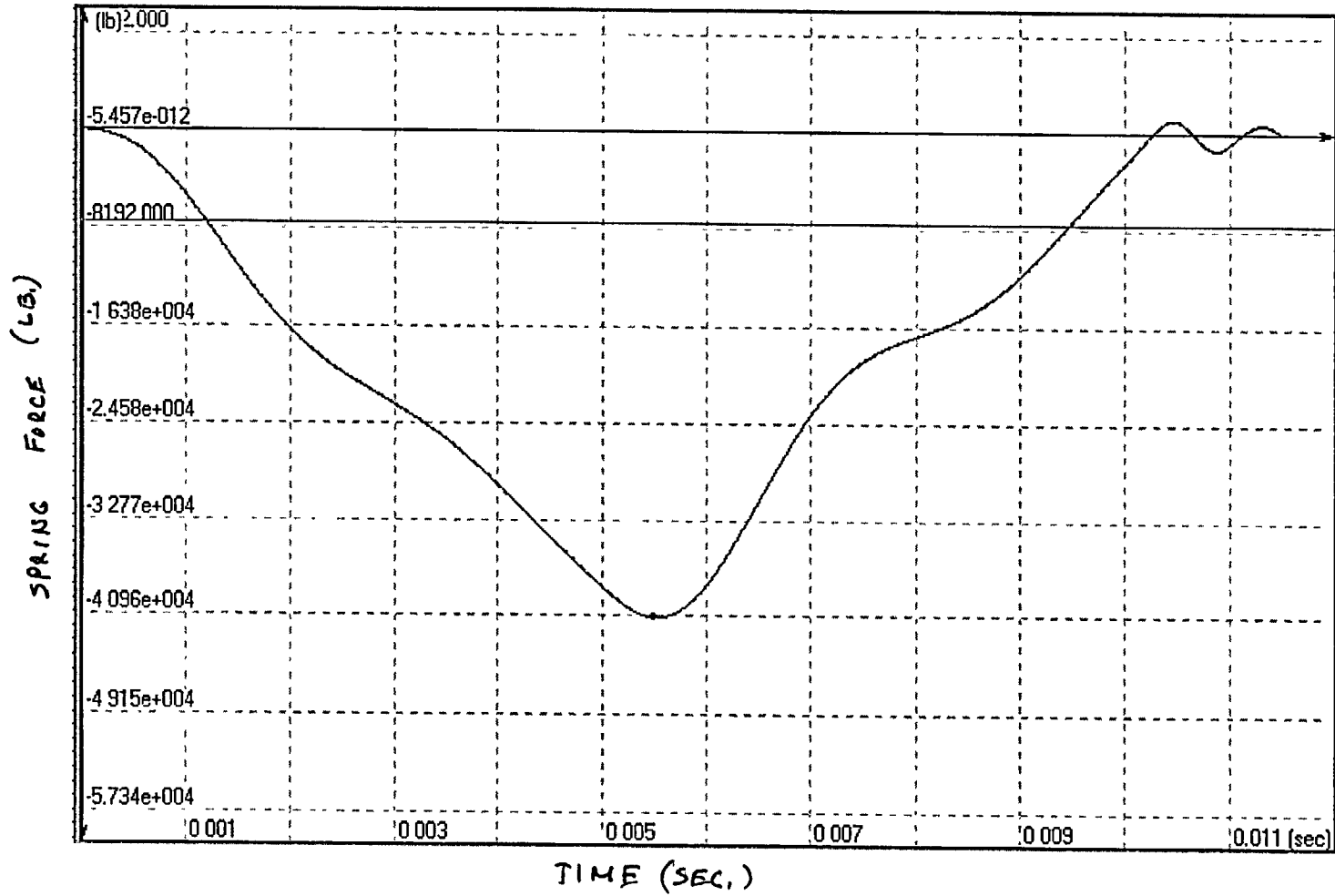


FIGURE 3.X.3; DYNAMIC MODEL FOR
 MULTI-DEGREE OF FREEDOM ANALYSIS
 FOR DLF DETERMINATION



HI-STORM FSAR
 HI-2002444

Fig. 3.X.4 Dynamic Force in Lower Panel Spring - PWR



HI-STORM FSAR
 HI-2002444

Fig. 3.X.5 Dynamic Force in Lower Panel Spring - BWR

APPENDIX 3.Y: MISCELLANEOUS CALCULATIONS

3.Y.1 CALCULATION FOR THE FILLET WELDS IN THE FUEL BASKET

The fillet welds in the fuel basket honeycomb are made by an autogenous operation that has been shown to produce highly consistent and porosity free weld lines. However, Subsection NG of the ASME Code permits only 40% quality credit on double fillet welds which can be only visually examined (Table NG-3352-1). Subsection NG, however, fails to provide a specific stress limit on such fillet welds. In the absence of a Code mandated limit, Holtec International's standard design procedure requires that the weld section possess as much load resistance capability as the parent metal section. Since the loading on the honeycomb panels is essentially that of section bending, it is possible to develop a closed form expression for the required weld throat t corresponding to panel thickness h .

We refer to Figure 3.Y.1 that shows a unit depth of panel-to-panel joint subjected to moment M .

The stress distribution in the panel is given by the classical Kirchoff beam formula

$$s_p = \frac{6M}{h^2}$$

or

$$M = \frac{s_p h^2}{6}$$

s_p is the extreme fiber stress in the panel.

Assuming that the panel edge-to-panel contact region develops no resistive pressure, Figure 3.Y.1(c) shows the free body of the dual fillet welds. F is the net compressive or tensile force acting on the surface of the leg of the weld.

From moment equilibrium

$$M = F(h + t)$$

Following standard weld design practice, we assume that the shear stress on the throat of the weld is equal to the force F divided by the weld throat area. If we assume 40% weld efficiency, minimum weld throat, and define S_w as the average shear stress on the weld throat, then for a unit depth of weld,

$$F = S_w (0.707) (0.4) t$$

$$F = 0.283 S_w t$$

Then, from Eq. 3.Y.2,

$$M = 0.283 S_w t (h+t)$$

Comparing the two foregoing expressions for M , we have

$$0.283 S_w (ht + t^2) = \frac{S_p h \sup 2}{6}$$

This is to be solved for the weld thickness t that is required for a panel thickness h . The relationship between S_p and S_w is evaluated using the most limiting hypothetical accident condition.

Specific stress levels appropriate for fillet welds for service conditions are found only in Subsection NF where 30% of the ultimate strength of the material is mandated (Table NF-3324.5(a)-1). For the Level D (faulted) condition appropriate to the most limiting drop or accident condition, Appendix F provides no specific limits for welds. Accordingly, Holtec set the weld stress limit for Level D conditions to be the weld stress limit for Level A conditions amplified by the ratio of the membrane stress limits set forth in Subsection NG for Level D and Level A, respectively.

Table 2.2.11 sets limits on S_p (primary membrane plus bending stress). Table 3.1.14 gives

$$S_p = 55,450 \text{ psi at } 725^\circ \text{ F}$$

The appropriate limit for the weld stress is set as

$$S_w = 0.42 S_u$$

Table 3.3.1 gives a value for the ultimate strength of the base metal as 62,350 psi at 725 degrees F. The weld metal used at the panel connections is one grade higher in ultimate tensile stress than the adjacent base metal (80,000 psi at room temperature compared with 75,000 for the base metal at room temperature).

The strength of the weld is assumed to decrease with temperature the same as the base metal.

$$S_w = .42 \times 80,000 \left(\frac{62,350}{75,000} \right) = 27,930 \text{ psi}$$

Therefore, the corresponding limit stress on the weld throat is

$$h^2 = (0.283) (6) \frac{S_w}{S_p} (ht + t^2)$$
$$h^2 = 1.698 \frac{S_w}{S_p} (ht + t^2)$$

The equation given above establishes the relationship between the weld size "t", the fuel basket panel wall thickness "h", and the ratio of allowable weld strength " S_w " to base metal allowable strength " S_p ". We now apply this formula to establish the minimum fillet weld size to be specified on the design drawings to insure a factor of safety of 1.0 subsequent to incorporation of the appropriate dynamic load amplifier. Table 3.4.6 gives fuel basket safety factors "SF" for primary membrane plus bending stress intensities corresponding to the base metal allowable strength S_p at 725 degrees F. As noted in Subsection 3.4.4.4.1, the reported safety factors are conservatively low because of the conservative assumptions in modeling. Appendix 3.X provides dynamic amplification factors "DAF" for each fuel basket type. To establish the minimum permissible weld size, S_p is replaced in the above formula by $(S_p \times (\text{DAF}/\text{SF} \times 1.1))$, and t/h computed for each basket. The additional 10% increase in safety factor is a conservative accounting that factors in the known conservatism in the

finite element solution and the results from the simplified evaluation in Subsection 3.4.4.4.1. The following results are obtained:

MINIMUM WELD SIZE FOR FUEL BASKETS					
Item	SF (Table 3.4.6) x 1.1	DAF (Appendix 3 X)	t/h	h (inch)	t (inch)
MPC-24	1.45	1.077	0.557	10/32	0.174
MPC-32	1.41	1.077	0.569	9/32	0.160
MPC-68	1.58	1.06	0.516	8/32	0.129

The minimum weld sizes in the above table do not apply to the welds that connect the cell angles to the primary cell plates in the MPC-24 basket. Based on the results of the finite element analysis described in Subsection 3.4.4.3.1.1, the minimum weld size at these locations is computed as

$$t_{\min} = \frac{\sqrt{2} \cdot q}{e \cdot S_w}$$

where q = maximum force per inch of weld = 436.7 lb/in (from finite element analysis)
 e = weld efficiency factor per ASME Subsection NG = 0.35
 S_w = allowable weld stress = 27,930 psi (see above)

Substituting these values into the above formula, we find

$$t_{\min} = 0.063in$$

Sheathing Weld Capacity

Theory:

Simple Force equilibrium relationships are used to demonstrate that the sheathing weld is adequate to support a 45g deceleration load applied vertically and horizontally to the sheathing and to the confined Boral. We perform the analysis assuming the weld is continuous and then modify the results to reflect the amplification due to intermittent welding.

Definitions

h = length of weld line (in.) (long side of sheathing)

w = width of weld line (in.) (short edge of sheathing)

t_w = weld size

e = 0.3 = quality factor for single fillet weld (from subsection NG, Table NG-3352-1)

W_b = weight of a Boral panel (lbf)

W_s = weight of sheathing confining a Boral panel (lbf)

G = 45

S_w = weld shear stress (psi)

Equations

Weld area = 2 (0.707 t_w e) (h) (neglect the top and bottom of the sheathing)

Load on weld = (W_b + W_s) G (either horizontal or vertical)

Weld stress from combined action of vertical plus horizontal load in each of the two directions.

$$S_w = \frac{G (W_b + W_s) \sqrt{3}}{2 (.707) e t_w (h)}$$

For a PWR panel, the weights are calculated as

$$W_b = 11.35 \text{ lb.}$$

$$W_s = 28.0 \text{ lb.}$$

The weld size is conservatively assumed as a 1/16" fillet weld, and the length and width of the weld line is

$$h = 156 \text{ in.}$$

$$w = 7.5 \text{ in.}$$

Therefore,

$$S_w = \frac{45 \times (11.35 + 28) \times 1.732}{1.414 \times 0.3 \times (1/16) (156)} = 742 \text{ psi}$$

For an MPC-68 panel, the corresponding values are

$$W_b = 7.56 \text{ lb.}$$

$$W_s = 17.48 \text{ lb.}$$

$$h = 139 \text{ in.}$$

$$w = 5 \text{ in.}$$

$$S_w = \frac{45 \times (7.56 + 17.48) \times 1.732}{1.414 \times 0.3 \times (1/16 \text{ in.}) (139 \text{ in.})} = 530 \text{ psi}$$

The actual welding specified along the length of a sheathing panel is 2" weld on 8" pitch. The effect of the intermittent weld is to raise the average weld shear stress by a factor of 4. From the above results, it is concluded that the sheathing weld stress is negligible during the most severe drop accident condition.

3.Y.2 Calculation for MPC Cover Plates in MPC Lid

The MPC cover plates are welded to the MPC lid during loading operations. The cover plates are part of the confinement boundary for the MPC. No credit is taken for the pressure retaining abilities of the quick disconnect couplings for the MPC vent and drain. Therefore, the MPC cover plates must meet ASME Code, Section III, Subsection NB limits for normal, off-normal, and accident conditions.

The normal and off-normal condition design basis MPC internal pressure is 100 psi. The accident condition design basis MPC internal pressure is 125 psi. Conservatively, the accident condition pressure loading is applied and it is demonstrated that the Level A limits for Subsection NB are met.

The MPC cover plate is depicted in the Design Drawings. The cover plate is stepped and has a maximum and minimum thickness of 0.38 inches and 0.1875 inches, respectively.

Conservatively, the minimum thickness is utilized for these calculations.

To verify the MPC cover plate maintains the MPC internal pressure while meeting the ASME Code, Subsection NB limits, the cover plate bending stress and shear stress, and weld stress are calculated and compared to allowables.

Definitions

P = accident condition MPC internal pressure (psi) = 125 psi

r = cover plate radius (in.) = 2 in.

t = cover plate minimum thickness (in.) = 0.1875 in.

t_w = weld size (in.) = 0.1875 in.

The design temperature of the MPC cover plate is conservatively taken as equal to the MPC lid, 550°F. The peak temperature of the MPC lid is experienced on the internal portion of the MPC lid, and the actual operating temperature of the top surface is less than 400°F.

For the design temperature of 550°F, the Alloy X allowable membrane stress intensity is

$$S_m = 16,950 \text{ psi}$$

The allowable weld shear stress is 0.3 S_u per Subsection NF of the ASME Code for Level A conditions.

Equations

Using Timoshenko, Strength of Materials, Part II, Advanced Theory and Problems, Third Edition, Page 99, the formula for the bending stress in the coverplate is:

$$S_b = \frac{(9.9)(P)(r^2)}{(8)(t^2)} \quad (\nu = 0.3)$$

$$S_b = \frac{(9.9)(125 \text{ psi})(2 \text{ in.})^2}{(8)(0.1875 \text{ in.})^2}$$

$$S_b = 17,600 \text{ psi}$$

The allowable bending stress is 1.5S_m.

Therefore, $S_b < 1.5S_m$ (i.e., 17,600 psi < 24,425 psi)

The shear stress due to the accident condition MPC internal pressure is calculated as follows:

$$\tau = \frac{P \pi r^2}{2 \pi r t}$$
$$\tau = \frac{(125 \text{ psi}) (\pi) (2 \text{ in})^2}{(2) (\pi) (2 \text{ in}) (0.1875 \text{ in})}$$
$$\tau = 667 \text{ psi}$$

This shear stress in the cover plate is less than the Level A limit of $0.4S_m = 6,780$ psi.

The stress in the weld is calculated by dividing the shear stress in the cover plate by 0.707 and applying a quality factor 0.3. The weld size is equal to the minimum cover plate thickness and therefore the weld stress can be calculated from the cover plate shear stress.

$$S_w = \frac{\tau}{0.707 \times 0.3} = \frac{667 \text{ psi}}{0.707 \times 0.3}$$
$$S_w = 3,145 \text{ psi}$$
$$S_w < 0.3 S_u = 0.3 \times 63,300 \text{ psi} = 18,990 \text{ psi}$$

The Level A weld stress limit of 30% of the ultimate strength (at 550°F) has been taken from Section NF of the ASME Code, the only section that specifically addresses stress limits for welds.

The stress developed as a result of the accident condition MPC internal pressure has been conservatively shown to be below the Level A, Subsection NB, ASME Code limits. The MPC cover plates meet the stress limits for normal, off-normal, and accident loading conditions at design temperature.

3.Y.3 Fuel Basket Angle Support Stress Calculations

The fuel basket internal to the MPC canister is supported by a combination of angle fuel basket supports and flat plate or solid bar fuel basket supports. These fuel basket supports are subject to significant load only when a lateral acceleration is applied to the fuel basket and the contained fuel. The quasi-static finite element analyses of the MPC's, under lateral inertia loading, focused on the structural details of the fuel basket and the MPC shell. Basket supports were modeled in less detail which served only to properly model the load transfer path between fuel basket and canister. Safety factors reported for the fuel basket supports from the finite element analyses, are overly conservative, and do not reflect available capacity of the fuel basket angle support. A more detailed stress analysis of the fuel basket angle supports is performed herein. We perform a strength of materials analysis of the fuel basket angle supports that complements the finite element results. We compute weld stresses at the support-to-shell interface, and membrane and bending stresses in the basket support angle plate itself. Using this strength of materials approach, we demonstrate that the safety factors for the fuel basket angle supports are larger than indicated by the finite element analysis.

The fuel basket supports of interest are angled plate components that are welded to the MPC shell using continuous single fillet welds. The design drawings and bill of materials in Section 1.5 of this submittal define the location of these supports for all MPC constructions. These basket supports experience no loading except when the fuel assembly basket and contained fuel is subject to lateral deceleration loads either from normal handling or accident events.

In this section, the analysis proceeds in the following manner. The fuel basket support loading is obtained by first computing the fuel basket weight (cell walls plus Boral plus sheathing) and adding to it the fuel weight. To maximize the support load, the MPC is assumed to be fully populated with fuel assemblies. This total calculated weight is then amplified by the design basis deceleration load and divided by the length of the fuel basket support. The resulting value is the load per unit length that must be resisted by all of the fuel basket supports. We next conservatively estimate, from the drawings for each MPC, the number of cells in a direct line (in the direction of the deceleration) that is resisted by the most highly loaded fuel basket angle support. We then compute the resisting load on the particular support induced by the inertia load from this number of cells. Force equilibrium on a simplified model of the fuel basket angle support then provides the weld load and the axial force and bending moment in the fuel basket support. The computation of safety factors is performed for a 45G load that bounds the non-mechanistic tip-over accident in HI-STORM and the deceleration load experienced by the MPC in a HI-TRAC side drop.

This section of Appendix 3.Y has been written using Mathcad; The notation "!=" is an equality.

We first establish as input data common to all MPC's, the allowable weld shear stress. In section 3.Y.1, the allowable weld stress for a Level D accident event defined. We further reduce this allowable stress by an appropriate weld efficiency obtained from the ASME Code, Section III, Subsection NG, Table NG-3352-1.

Weld efficiency $e := 0.35$ (single fillet weld, visual inspection only)

The fuel support brackets are constructed from Alloy "X". At the canister interface,

Ultimate Strength $S_u := 64000 \cdot \text{psi}$ Alloy X @ 450 degrees F (Table 3.3.1)

Note that here we use the design temperature for the MPC shell under normal conditions (Table 2.2.3) since the fire accident temperature is not applicable during the tip-over. The allowable weld shear stress, incorporating the weld efficiency is (use the base metal ultimate strength for additional conservatism) determined as:

$\tau_{all} := .42 \cdot S_u \cdot e$ $\tau_{all} = 9.408 \times 10^3 \text{ psi}$

For the non-mechanistic tip-over, the design basis deceleration in "g's" is

$G := 45$ (Table 3.1.2)

The total load to be resisted by the fuel basket supports is obtained by first computing the moving weight, relative to the MPC canister, for each MPC. The fuel basket weight is obtained from the weight calculation (dated 11/11/97) in HI-971656, HI-STAR 100 Structural Calculation Package.

The weights of the fuel baskets and total fuel load are (the notation "lbf" = "pound force")

Fuel Basket	Fuel		
$W_{mpc32} := 11875 \cdot \text{lbf}$	$W_{f32} := 53760 \cdot \text{lbf}$	MPC-32	
$W_{mpc68} := 15263 \cdot \text{lbf}$	$W_{f68} := 47600 \cdot \text{lbf}$	MPC-68	
$W_{mpc24} := 17045 \cdot \text{lbf}$	$W_{f24} := 40320 \cdot \text{lbf}$	MPC-24	
$W_{mpc24e} := 21496 \cdot \text{lbf}$	$W_{f24} := 40320 \cdot \text{lbf}$	MPC-24E	

Since the MPC-24E is heavier, we assign a bounding weight to the MPC-24 basket equal to that of the MPC-24E in the following calculation. |

$W_{mpc24} := W_{mpc24e}$ |

The minimum length of the fuel basket support is $L := 168 \cdot \text{in}$

Note that for the MPC-68, the support length is increased by 1/2"

Therefore, the load per unit length that acts along the line of action of the deceleration, and is resisted by the total of all supports, is computed as

$$Q_{32} := \frac{(W_{\text{mpc}32} + W_{f32}) \cdot G}{(L + 0.5 \cdot \text{in})} \quad Q_{32} = 1.753 \times 10^4 \frac{\text{lb}}{\text{in}}$$

$$Q_{68} := \frac{(W_{\text{mpc}68} + W_{f68}) \cdot G}{(L + 0.5 \cdot \text{in})} \quad Q_{68} = 1.679 \times 10^4 \frac{\text{lb}}{\text{in}}$$

$$Q_{24} := \frac{(W_{\text{mpc}24} + W_{f24}) \cdot G}{L} \quad Q_{24} = 1.656 \times 10^4 \frac{\text{lb}}{\text{in}}$$

$$Q_{24e} := \frac{(W_{\text{mpc}24e} + W_{f24}) \cdot G}{L} \quad Q_{24e} = 1.656 \times 10^4 \frac{\text{lb}}{\text{in}}$$

The subscript associated with the above items is used as the identifier for the particular MPC.

An examination of the MPC design drawings in Section 1.5 indicates that the deceleration load is supported by shims and by fuel basket angle supports. By inspection of the relevant drawing, we can determine that the most highly loaded fuel basket angle support will resist the deceleration load from "NC" cells where NC for each basket type is obtained by counting the cells and portions of cells "above" the support in the direction of the deceleration. The following values for NC are used in the subsequent computation of fuel basket angle support stress:

$$NC_{32} := 6 \quad NC_{68} := 8 \quad NC_{24} := 7$$

The total normal load per unit length on the fuel basket support for each MPC type is therefore computed as:

$$P_{32} := Q_{32} \cdot \frac{NC_{32}}{32} \qquad P_{32} = 3.287 \times 10^3 \frac{\text{lbf}}{\text{in}}$$

$$P_{68} := Q_{68} \cdot \frac{NC_{68}}{68} \qquad P_{68} = 1.975 \times 10^3 \frac{\text{lbf}}{\text{in}}$$

$$P_{24} := Q_{24} \cdot \frac{NC_{24}}{24} \qquad P_{24} = 4.829 \times 10^3 \frac{\text{lbf}}{\text{in}}$$

$$P_{24e} := Q_{24e} \cdot \frac{NC_{24}}{24} \qquad P_{24e} = 4.829 \times 10^3 \frac{\text{lbf}}{\text{in}}$$

Here again, the subscript notation identifies the particular MPC.

Figure 3.Y.2 shows a typical fuel basket support with the support reactions at the base of the leg. The applied load and the loads necessary to put the support in equilibrium is not subscripted since the figure is meant to be typical of any MPC fuel basket angle support. The free body is drawn in a conservative manner by assuming that the load P is applied at the quarter point of the top flat portion. In reality, as the load is applied, the top flat portion deforms and the load shifts completely to the outer edges of the top flat section of the support. From the design drawings, we use the appropriate dimensions and perform the following analyses (subscripts are introduced as necessary as MPC identifiers):

The free body diagram shows the bending moment that will arise at the location where the idealized top flat section and the angled support are assumed to meet. Compatibility of joint rotation at the connection between the top flat and the angled portion of the support plus force and moment equilibrium equations from classical beam theory provide sufficient equations to solve for the bending moment at the connection (point O in Figure 3.Y.2), the load R at the weld, and the bending moment under the load P/2.

$$M_o := \frac{9}{16} \cdot \frac{P_w^2}{(S + 3 \cdot w)} \quad \blacksquare$$

Note that the small block after the equation indicates that this is a text equation rather than an evaluated equation. This is a Mathcad identifier.

The load in the weld, R, is expressed in the form

$$R := \frac{P \cdot H}{2 \cdot L} + \frac{M_o}{L}$$

Finally, the bending moment under the load, on the top flat portion, is given as

$$M_p := \frac{P}{2} \cdot \frac{w}{2} - M_o$$

The throat thickness of the fillet weld used between the supports and the MPC shell is

$$t_w := 0.125 \cdot \text{in} \cdot 7071$$

The wall thickness for computation of member stresses is:

$$t_{\text{wall}} := \frac{5}{16} \cdot \text{in}$$

Performing the indicated computations and evaluations for each of the MPC's gives:

MPC-32

$$\theta_{32} := 9 \cdot \text{deg} \quad L_{32} := 5.6 \cdot \text{in} \quad w_{32} := \left(0.25 + .125 + .5 \cdot \frac{5}{16} \right) \cdot \text{in}$$

Therefore

$$H_{32} := L_{32} \cdot \tan(\theta_{32}) \quad H_{32} = 0.887 \text{ in} \quad w_{32} = 0.531 \text{ in}$$

$$S := \sqrt{L_{32}^2 + H_{32}^2} \quad S = 5.67 \text{ in}$$

$$M_o := \frac{9}{16} \cdot \frac{(P_{32} \cdot w_{32}^2)}{(S + 3 \cdot w_{32})} \quad M_o = 71.832 \text{ lbf} \cdot \frac{\text{in}}{\text{in}}$$

$$R_{32} := \frac{P_{32} \cdot H_{32}}{2 \cdot L_{32}} + \frac{M_o}{L_{32}} \quad R_{32} = 273.102 \frac{\text{lbf}}{\text{in}}$$

$$M_p := \frac{P_{32}}{2} \cdot \frac{w_{32}}{2} - M_o \quad M_p = 364.672 \text{ lbf} \cdot \frac{\text{in}}{\text{in}}$$

The weld stress is

$$\tau_{\text{weld}} := \frac{R_{32}}{t_w} \quad \tau_{\text{weld}} = 3.09 \times 10^3 \text{ psi}$$

For this event, the safety factor on the weld is

$$SF_{\text{weld}} := \frac{\tau_{\text{all}}}{\tau_{\text{weld}}} \quad SF_{\text{weld}} = 3.045$$

The maximum bending stress in the angled member is

$$\sigma_{\text{bending}} := 6 \cdot \frac{M_o}{t_{\text{wall}}^2} \quad \sigma_{\text{bending}} = 4.413 \times 10^3 \text{ psi}$$

The direct stress in the basket support angled section is

$$\sigma_{\text{direct}} := \frac{(R_{32} \cdot \sin(\theta_{32}) + .5 \cdot P_{32} \cdot \cos(\theta_{32}))}{t_{\text{wall}}} \quad \sigma_{\text{direct}} = 5.331 \times 10^3 \text{ psi}$$

From Table 3.1.16, the allowable membrane stress intensity for this condition is

$$S_{\text{membrane}} := 39400 \cdot \text{psi} \quad (\text{use the value at 600 degree F to conservatively bound the Safety Factor})$$

$$SF_{\text{membrane}} := \frac{S_{\text{membrane}}}{\sigma_{\text{direct}}} \quad SF_{\text{membrane}} = 7.391$$

From Table 3.1.16, the allowable combined stress intensity for this accident condition is

$$S_{\text{combined}} := 59100 \cdot \text{psi} \quad (\text{use the value at 600 degree F to conservatively bound the Safety Factor})$$

$$SF_{\text{combined}} := \frac{S_{\text{combined}}}{\sigma_{\text{direct}} + \sigma_{\text{bending}}} \quad SF_{\text{combined}} = 6.065$$

Note that for this model, it is appropriate to compare the computed stress with allowable stress intensities since we are dealing with beams and there are no surface pressure stresses.

The maximum bending stress in the top flat section is

$$\sigma_{\text{bending}} := 6 \cdot \frac{M_p}{t_{\text{wall}}^2} \quad \sigma_{\text{bending}} = 2.241 \times 10^4 \text{ psi}$$

The direct stress in the basket support top flat section is

$$\sigma_{\text{direct}} := \frac{R_{32}}{t_{\text{wall}}} \quad \sigma_{\text{direct}} = 873.926 \text{ psi}$$

Computing the safety factors gives:

$$SF_{\text{membrane}} := \frac{S_{\text{membrane}}}{\sigma_{\text{direct}}} \quad SF_{\text{membrane}} = 45.084$$

$$SF_{\text{combined}} := \frac{S_{\text{combined}}}{\sigma_{\text{direct}} + \sigma_{\text{bending}}} \quad SF_{\text{combined}} = 2.539$$

All safety factors are greater than 1.0; therefore, the design is acceptable

MPC-24

$$\theta_{24} := 9 \cdot \text{deg} \quad L_{24} := 4 \cdot \text{in} \quad w_{24} := \left(0.25 + .125 + .5 \cdot \frac{5}{16} \right) \cdot \text{in}$$

Therefore

$$H_{24} := L_{24} \cdot \tan(\theta_{24}) \quad H_{24} = 0.634 \text{ in} \quad w_{24} = 0.531 \text{ in}$$

$$S := \sqrt{L_{24}^2 + H_{24}^2} \quad S = 4.05 \text{ in}$$

$$M_o := \frac{9}{16} \cdot \frac{(P_{24} \cdot w_{24}^2)}{(S + 3 \cdot w_{24})} \quad M_o = 135.848 \text{ lbf} \cdot \frac{\text{in}}{\text{in}}$$

$$R_{24} := \frac{P_{24} \cdot H_{24}}{2 \cdot L_{24}} + \frac{M_o}{L_{24}} \quad R_{24} = 416.411 \frac{\text{lbf}}{\text{in}}$$

$$M_p := \frac{P_{24}}{2} \cdot \frac{w_{24}}{2} - M_o \quad M_p = 505.553 \text{ lbf} \cdot \frac{\text{in}}{\text{in}}$$

The weld stress is

$$\tau_{\text{weld}} := \frac{R_{24}}{t_w} \quad \tau_{\text{weld}} = 4.711 \times 10^3 \text{ psi}$$

For this event, the safety factor on the weld is

$$SF_{\text{weld}} := \frac{\tau_{\text{all}}}{\tau_{\text{weld}}} \quad SF_{\text{weld}} = 1.997$$

The maximum bending stress in the angled member is

$$\sigma_{\text{bending}} := 6 \cdot \frac{M_o}{t_{\text{wall}}^2} \quad \sigma_{\text{bending}} = 8.347 \times 10^3 \text{ psi}$$

The direct stress in the basket support angled section is

$$\sigma_{\text{direct}} := \frac{(R_{24} \cdot \sin(\theta_{24}) + .5 \cdot P_{24} \cdot \cos(\theta_{24}))}{t_{\text{wall}}} \quad \sigma_{\text{direct}} = 7.84 \times 10^3 \text{ psi}$$

From Table 3.1.16, the allowable membrane stress intensity for this condition is

$$S_{\text{membrane}} := 39400 \cdot \text{psi} \quad (\text{use the value at 600 degree F to conservatively bound the Safety Factor})$$

$$SF_{\text{membrane}} := \frac{S_{\text{membrane}}}{\sigma_{\text{direct}}} \quad SF_{\text{membrane}} = 5.025$$

From Table 3.1.16, the allowable combined stress intensity for this accident condition is

$$S_{\text{combined}} := 59100 \cdot \text{psi} \quad (\text{use the value at 600 degree F to conservatively bound the Safety Factor})$$

$$SF_{\text{combined}} := \frac{S_{\text{combined}}}{\sigma_{\text{direct}} + \sigma_{\text{bending}}} \quad SF_{\text{combined}} = 3.651$$

Note that for this model, it is appropriate to compare the computed stress with allowable stress intensities since we are dealing with beams and there are no surface pressure stresses.

$$SF_{\text{membrane}} := \frac{S_{\text{membrane}}}{\sigma_{\text{direct}}} \quad SF_{\text{membrane}} = 5.025$$

$$SF_{\text{combined}} := \frac{S_{\text{combined}}}{\sigma_{\text{direct}} + \sigma_{\text{bending}}} \quad SF_{\text{combined}} = 3.651$$

The maximum bending stress in the top flat section is

$$\sigma_{\text{bending}} := 6 \cdot \frac{M_p}{t_{\text{wall}}^2} \quad \sigma_{\text{bending}} = 3.106 \times 10^4 \text{ psi}$$

The direct stress in the basket support top flat section is

$$\sigma_{\text{direct}} := \frac{R_{24}}{t_{\text{wall}}} \quad \sigma_{\text{direct}} = 1.333 \times 10^3 \text{ psi}$$

Computing the safety factors gives:

$$SF_{\text{membrane}} := \frac{S_{\text{membrane}}}{\sigma_{\text{direct}}} \quad SF_{\text{membrane}} = 29.568$$

$$SF_{\text{combined}} := \frac{S_{\text{combined}}}{\sigma_{\text{direct}} + \sigma_{\text{bending}}} \quad SF_{\text{combined}} = 1.824$$

All safety factors are greater than 1.0; therefore, the design is acceptable

MPC-68

$$\theta_{68} := 12.5 \cdot \text{deg} \quad L_{68} := 4.75 \cdot \text{in} \quad (\text{estimated}) \quad w_{68} := \left(0.75 - .5 \cdot \frac{5}{16} \right) \cdot \text{in}$$

Note that in the MPC-68, there is no real top flat portion to the angle support. "w" is computed as the radius of the bend less 50% of the wall thickness. However, in the remaining calculations, the applied load is assumed a distance w/2 from the center on each side of the support centerline in Figure 3.Y 2.

Therefore

$$H_{68} := L_{68} \cdot \tan(\theta_{68}) \quad H_{68} = 1.053 \text{ in} \quad w_{68} = 0.594 \text{ in}$$

$$S := \sqrt{L_{68}^2 + H_{68}^2} \quad S = 4.865 \text{ in}$$

$$M_o := \frac{9}{16} \cdot \frac{P_{68} \cdot w_{68}^2}{(S + 3 \cdot w_{68})} \quad M_o = 58.928 \text{ lbf} \cdot \frac{\text{in}}{\text{in}}$$

$$R_{68} := \frac{P_{68} \cdot H_{68}}{2 \cdot L_{68}} + \frac{M_o}{L_{68}} \quad R_{68} = 231.34 \frac{\text{lbf}}{\text{in}}$$

$$M_p := \frac{P_{68}}{2} \cdot \frac{w_{68}}{2} - M_o \quad M_p = 234.251 \text{ lbf} \cdot \frac{\text{in}}{\text{in}}$$

The weld stress is

$$\tau_{\text{weld}} := \frac{R_{68}}{t_w} \quad \tau_{\text{weld}} = 2.617 \times 10^3 \text{ psi}$$

The safety factor on the weld is

$$SF_{\text{weld}} := \frac{\tau_{\text{all}}}{\tau_{\text{weld}}} \quad SF_{\text{weld}} = 3.594$$

The maximum bending stress in the angled member is

$$\sigma_{\text{bending}} := 6 \cdot \frac{M_o}{t_{\text{wall}}^2} \quad \sigma_{\text{bending}} = 3.621 \times 10^3 \text{ psi}$$

The direct stress in the basket support angled section is

$$\sigma_{\text{direct}} := \frac{(R_{68} \cdot \sin(\theta_{68}) + .5 \cdot P_{68} \cdot \cos(\theta_{68}))}{t_{\text{wall}}} \quad \sigma_{\text{direct}} = 3.245 \times 10^3 \text{ psi}$$

$$SF_{\text{membrane}} := \frac{S_{\text{membrane}}}{\sigma_{\text{direct}}} \quad SF_{\text{membrane}} = 12.14$$

$$SF_{\text{combined}} := \frac{S_{\text{combined}}}{\sigma_{\text{direct}} + \sigma_{\text{bending}}} \quad SF_{\text{combined}} = 8.608$$

The maximum bending stress in the idealized top flat section is

$$\sigma_{\text{bending}} := 6 \cdot \frac{M_p}{t_{\text{wall}}^2} \quad \sigma_{\text{bending}} = 1.439 \times 10^4 \text{ psi}$$

The direct stress in the basket support top flat section is

$$\sigma_{\text{direct}} := \frac{R_{68}}{t_{\text{wall}}} \quad \sigma_{\text{direct}} = 740.289 \text{ psi}$$

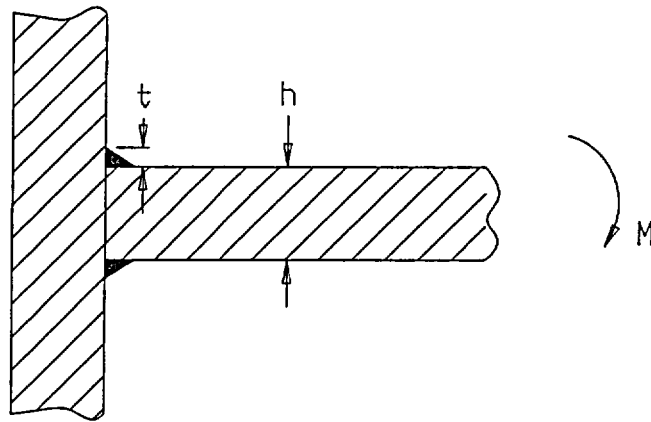
$$SF_{\text{membrane}} := \frac{S_{\text{membrane}}}{\sigma_{\text{direct}}} \quad SF_{\text{membrane}} = 53.222$$

$$SF_{\text{combined}} := \frac{S_{\text{combined}}}{\sigma_{\text{direct}} + \sigma_{\text{bending}}} \quad SF_{\text{combined}} = 3.905$$

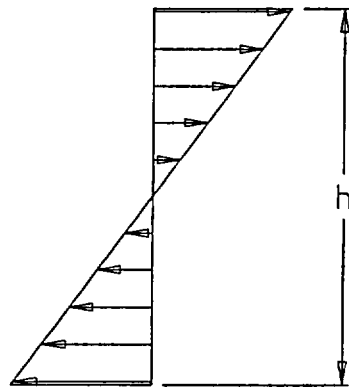
All safety factors are greater than 1.0; therefore, the design is acceptable

SUMMARY OF RESULTS

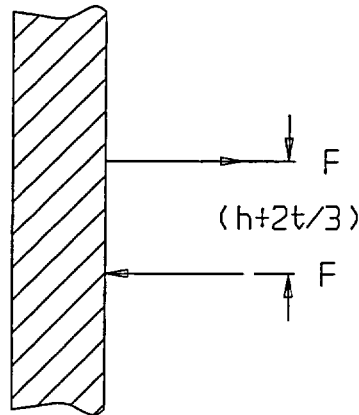
The above calculations demonstrate that for all MPC fuel basket angle supports, the minimum safety margin is 1.82 (MPC-24 combined membrane plus bending in the top flat section). This is a larger safety factor than predicted from the finite element solution. The reason for this increase is attributed to the fact that the finite element analysis used a less robust structural model of the supports for stress analysis purposes since the emphasis there was on analysis of the fuel basket itself and the MPC canister. Therefore, in reporting safety factors, or safety margins, the minimum safety factor of 1.82 should be used for this component in any summary table.



(a) Loading Configuration

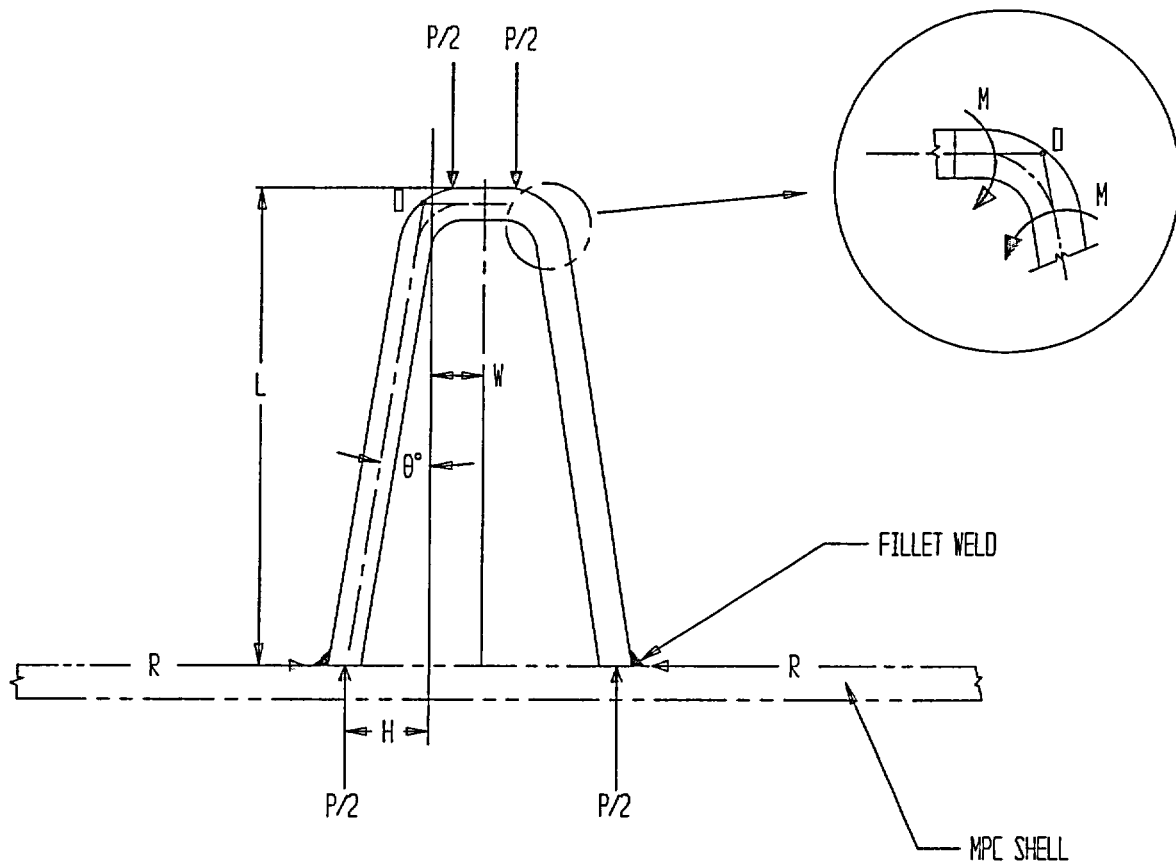


(b) Bending Stress in the Panel



(c) Reaction in the Welds

FIGURE 3.Y.1; FREEBODY OF STRESS DISTRIBUTION IN THE WELD AND THE HONEYCOMB PANEL



$$S^2 = L^2 + H^2$$

WHERE
 S = LENGTH OF ANGLED SECTION

FIGURE 3.Y.2: FREEBODY OF IDEALIZED FUEL BASKET SUPPORT

APPENDIX 3.Z HI-TRAC HORIZONTAL DROP ANALYSIS

3.Z.1 Introduction

This appendix considers the horizontal drop of a fully loaded HI-TRAC transfer cask from a transport vehicle. A maximum drop height (height of lowest point of HI-TRAC above the target surface) is postulated. The purpose of the analysis is to determine the decelerations that arise from target impact.

3.Z.2 References

[3.Z.1] Young, Warren C., Roark's Formulas for Stress and Strain, 6th Edition, McGraw-Hill, 1989.

[3.Z.2] Working Model, v.4.0, Knowledge Revolution, 1998.

[3.Z.3] Appendix 3.AL of HI-951312, Revision 5.

3.Z.3 Composition

This appendix was created using the Mathcad (version 8) software package. Mathcad uses the symbol ':=' as an assignment operator, and the equals symbol '=' retrieves values for constants or variables. Mathcad's built-in equation solver is also used.

3.Z.4 General Assumptions

1. Formulae taken from Reference 3.Z.1 are based on assumptions that are delineated in that reference.
2. Structural damping in HI-TRAC is neglected.
3. HI-TRAC is modeled as a rigid body for the purpose of simulating its behavior under a horizontal free drop.
4. The impacted foundation is conservatively assumed to respond as a linearly elastic spring. Spring constants are calculated in [3.Z.3].
5. The energy absorbing capacity and any structural resistance of the water jacket is conservatively neglected.

3.Z.5 Methodology

A dynamic model of the HI-TRAC transfer cask is constructed. The dynamic model also includes a foundation stiffness at each end of the system where impacts occur in the event of a handling accident. This appendix contains the following calculations:

- a) Assuming the HI-TRAC behaves like a free-free beam, calculate the lowest natural frequency of the HI-TRAC. The purpose of this calculation is to buttress the assumption that a rigid body model of HI-TRAC is sufficient for the global dynamic analysis.
- b) Use the dynamic simulation code Working Model [3.Z.2], with conservative estimates of stiffness to perform a simulation of the handling accident. Because of the geometry of the transfer lid, initial impact occurs at the transfer lid (or pocket trunnion) with subsequent rotation of the transfer cask, and then a secondary impact occurs at the top of the cask.
- c) To maximize the computed decelerations, the maximum stiffness predicted at any location is used in the model. However, to provide conservative results, the minimum impact damping value at the same location is utilized. Appendix 3.AL provides the necessary calculations and results to determine the appropriate values for the dynamic model.
- e) Demonstrate by calculation of the maximum bending stress in the outer shell of HI-TRAC, that ASME Code Level D stress limits are maintained under the limiting g loading. The inner shell will have lower stress levels.

3.Z.6 Input Data - HI-TRAC 125

All input dimensions are obtained from Holtec drawing no. 1880.

Drop height (arbitrarily chosen as upper limit)	$H := 50 \cdot \text{in}$
Outside diameter of outer shell	$D_o := 81.25 \cdot \text{in}$
Inside diameter of inner shell	$D_i := 68.75 \cdot \text{in}$
Thickness of outer shell	$t_o := 1 \cdot \text{in}$
Thickness of inner shell	$t_i := 0.75 \cdot \text{in}$

Maximum unsupported length between contact locations with ground $L := 190 \cdot \text{in}$

The following parameters are taken from Chapter 3 of the HI-STORM FSAR.

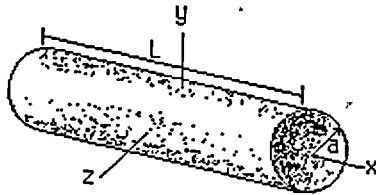
125-ton HI-TRAC bounding dry weight (Table 3.2.2) $W := 243000 \cdot \text{lb}$

Young's Modulus SA-516-Gr70 @ 350 deg. F (Table 3.3.2) $E := 28 \cdot 10^6 \cdot \text{psi}$

Allowable membrane stress intensity for Level D condition @ 350 deg. F for SA-516-Gr70 (Table 3.1.12) $S_a := 39750 \cdot \text{psi}$

Maximum Deceleration g level (Table 3.1.2) $G_{\text{max}} := 45$

Calculation of mass moment of inertia for simulation



HI TRAC 125

$$L := 201 \cdot \text{in} \quad a := \frac{94}{2} \cdot \text{in} \quad \text{mass} := \frac{243000}{g} \cdot \text{lb} \quad \text{mass} = 2.43 \times 10^5 \text{ lb}$$

The outer dimension of the water jacket is used for mass moment of inertia calculation.

$$I_y := \frac{1}{12} \cdot \text{mass} \cdot (3 \cdot a^2 + L^2) \quad \text{Moment about } y$$

$$I_y = 2.055 \times 10^5 \text{ lb} \cdot \text{ft} \cdot \text{sec}^2 \quad I_y = 9.523 \times 10^8 \text{ lb} \cdot \text{in}^2$$

3.Z.7 Calculation of Lowest Natural Frequency of HI-TRAC-125

It is assumed that HI-TRAC contacts the ground only at the ends since there is a protruding hard point at the lower end (either the rotation trunnion, or the transfer lid support rails. Once the lower end hard point contacts the ground, the other end of HI-TRAC (either the water jacket or the top flange, will contact ground. In order to provide a basis for development of a dynamic model of the HI-TRAC handling event, the lowest natural frequency of a free-free beam is computed. The purpose of this calculation is simply to show that the lowest frequency in a beam mode is less than 33 Hz.

Calculate the area moment of inertia of the inner and outer shells of HI-TRAC

$$d_o := D_o - t_o \quad d_o = 80.25 \text{ in} \quad d_{125} := d_o$$

$$d_i := D_i + t_i \quad d_i = 69.5 \text{ in}$$

The moment of inertia is calculated from the equation

$$I := \pi \cdot t_i \cdot \left(\frac{d_i}{2}\right)^3 + \pi \cdot t_o \cdot \left(\frac{d_o}{2}\right)^3 \quad I = 3.018 \times 10^5 \text{ in}^4 \quad I_{125} := I$$

Next, the weight per unit of unsupported length is computed as,

$$w := \frac{W}{L} \quad w = 1.209 \times 10^3 \frac{\text{lbf}}{\text{in}}$$

In terms of these computed quantities, the first natural frequency is given as [3.Z.1, Table 36, Case 4]:

$$f_1 := \frac{22.4}{2 \cdot \pi} \cdot \sqrt{\frac{E \cdot I \cdot g}{w \cdot L^4}} \quad f_1 = 144.968 \text{ Hz}$$

Using the same reference [3.Z.1], the second mode frequency that would be excited in the free drop has a natural frequency equal to

$$f_2 := \frac{61.7}{22.4} \cdot f_1 \quad f_2 = 399.308 \text{ Hz}$$

The natural frequencies calculated above are in the rigid range ($> 33 \text{ Hz}$). Therefore, simulation of HI-TRAC as a rigid body in any dynamic analysis is appropriate.

3.Z.9 Simulation of the Free Drop - HI-TRAC 125

For the specified free drop, the velocity of HI-TRAC at the instant of contact is

$$V_0 := \sqrt{2 \cdot g \cdot H} \quad V_0 = 196.491 \frac{\text{in}}{\text{sec}}$$

Figure 3.Z.1 shows the drop model and the results for accelerations using Working Model. Primary and secondary impact magnitudes of the accelerations at the two ends are reported as well as the magnitude of the vertical deceleration of the mass center of the rigid body representing HI-TRAC. Figures 3.Z.3, 3.Z.5, and 3.Z.6 show the input screens for the parameters required for the analysis. From Figure 3.Z.1, the following results can be determined:

Bottom deceleration at primary impact

$$a_{bp} := 12610 \cdot \frac{\text{in}}{\text{sec}^2}$$

$$\text{Max_gp} := \frac{a_{bp}}{g}$$

$$\text{Max_gp} = 32.661$$

Top deceleration at secondary impact

$$a_{ts} := 10320 \cdot \frac{\text{in}}{\text{sec}^2}$$

$$\text{Max_gs} := \frac{a_{ts}}{g}$$

$$\text{Max_gs} = 26.73$$

The maximum deceleration at the mass center is

$$A_{ms} := 7650 \cdot \frac{\text{in}}{\text{sec}^2}$$

The maximum impact force at either end is bounded by

$$F_{\text{impact_125}} := \frac{W}{g} \cdot A_{ms}$$

$$F_{\text{impact_125}} = 4.815 \times 10^6 \text{ lbf}$$

3.Z.10 Input Data - HI-TRAC 100

All input dimensions are obtained from Holtec drawing no. 2145.

Drop height	H := 50·in
Outside diameter of outer shell	D _o := 78.125·in
Inside diameter of inner shell	D _i := 68.75·in
Thickness of outer shell	t _o := 1·in
Thickness of inner shell	t _i := 0.75·in
Maximum unsupported length between contact locations with ground	L := 190·in

The following parameters are taken from Chapter 3 of the HI-STORM FSAR.

100-ton HI-TRAC bounding dry weight (Table 3.2.2)	W := 201000·lbf
Young's Modulus SA-516-Gr70 @ 350 deg. F (Table 3.3.2)	E := 28·10 ⁶ ·psi
Allowable membrane stress intensity for Level D condition @ 350 deg. F for SA-516-Gr70 (Table 3.1.12)	S _{l_a} := 39750·psi
Maximum Deceleration g level (Table 3.1.2)	G _{max} := 45

Calculation of mass and mass moment of inertia for HI-TRAC 100

$$L := 201 \cdot \text{in} \quad a := \frac{91}{2} \cdot \text{in} \quad \text{mass} := \frac{201000}{g} \cdot \text{lbf} \quad \text{mass} = 2.01 \times 10^5 \text{ lb}$$

The outer dimension of the water jacket is used for mass moment of inertia calculation.

$$I_y := \frac{1}{12} \cdot \text{mass} \cdot (3 \cdot a^2 + L^2) \quad \text{Moment about } y \quad I_y = 7.807 \times 10^8 \text{ lb} \cdot \text{in}^2$$

3.Z.7 Calculation of Lowest Natural Frequency of HI-TRAC-100

It is assumed that HI-TRAC contacts the ground only at the ends since there is a protruding hard point at the lower end (either the rotation trunnion, or the transfer lid support rails). Once the lower end hard point contacts the ground, the other end of HI-TRAC (either the water jacket or the top flange, will contact ground. In order to provide a basis for development of a dynamic model of the HI-TRAC handling event, the lowest natural frequency of a free-free beam is computed. The purpose of this calculation is simply to show that the lowest frequency in a beam mode is less than 33 Hz.

Calculate the area moment of inertia of the inner and outer shells of HI-TRAC

$$d_o := D_o - t_o \quad d_o = 77.125 \text{ in} \quad d_{100} := d_o$$

$$d_i := D_i + t_i \quad d_i = 69.5 \text{ in}$$

The moment of inertia is calculated from the equation

$$I := \pi \cdot t_i \cdot \left(\frac{d_i}{2}\right)^3 + \pi \cdot t_o \cdot \left(\frac{d_o}{2}\right)^3 \quad I = 2.79 \times 10^5 \text{ in}^4 \quad I_{100} := I$$

Next, the weight per unit of unsupported length is computed as,

$$w := \frac{W}{L} \quad w = 1 \times 10^3 \frac{\text{lbf}}{\text{in}}$$

In terms of these computed quantities, the first natural frequency is given as [3.Z.1, Table 36, Case 4]:

$$f_1 := \frac{22.4}{2 \cdot \pi} \cdot \sqrt{\frac{E \cdot I \cdot g}{w \cdot L^4}} \quad f_1 = 153.258 \text{ Hz}$$

Using the same reference [3.Z.1], the second mode frequency that would be excited in the free drop has a natural frequency equal to

$$f_2 := \frac{61.7}{22.4} \cdot f_1 \quad f_2 = 422.142 \text{ Hz}$$

The natural frequencies calculated above are in the rigid range (> 33 Hz). Therefore, simulation of HI-TRAC as a rigid body in any dynamic analysis is appropriate.

3.Z.11 Simulation of the Free Drop - HI-TRAC 100

For the specified free drop, the velocity of HI-TRAC at the instant of contact is

$$V_0 := \sqrt{2 \cdot g \cdot H} \quad V_0 = 196.491 \frac{\text{in}}{\text{sec}}$$

Figure 3.Z.2 shows the drop model and the results for accelerations using Working Model. Primary and secondary impact magnitudes of the accelerations at the two ends are reported as well as the magnitude of the vertical deceleration of the mass center of the rigid body representing HI-TRAC. Figure 3.Z.4 shows the properties of the rigid body used to simulate the cask. The following results are obtained:

$$\text{Bottom deceleration at primary impact} \quad a_{bp} := 12810 \cdot \frac{\text{in}}{\text{sec}^2}$$

$$\text{Max_gp} := \frac{a_{bp}}{g} \quad \text{Max_gp} = 33.179$$

$$\text{Top deceleration at secondary impact} \quad a_{ts} := 10440 \cdot \frac{\text{in}}{\text{sec}^2}$$

$$\text{Max_gs} := \frac{a_{ts}}{g} \quad \text{Max_gs} = 27.04$$

The maximum deceleration at the mass center is

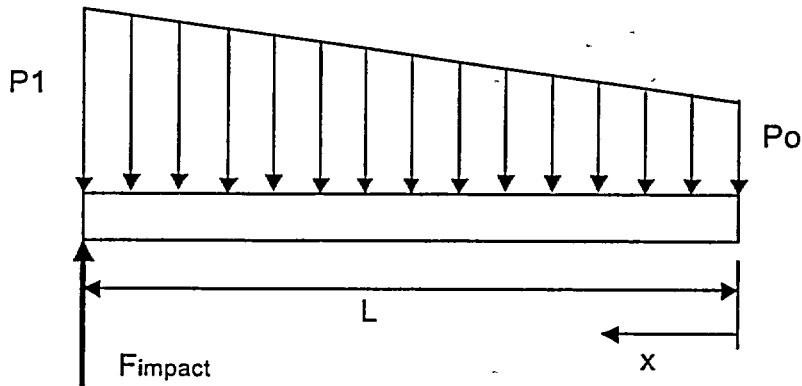
$$A_{ms} := 7361 \cdot \frac{\text{in}}{\text{sec}^2}$$

The maximum impact force at either end is bounded by

$$F_{\text{impact_100}} := \frac{W}{g} \cdot A_{ms} \quad F_{\text{impact_100}} = 3.832 \times 10^6 \text{ lbf}$$

3.Z.12 Maximum Axial Stress in HI-TRAC Under the Lateral Deceleration.

At the instant when the maximum impact force occurs, a distributed inertia force balances the impact load. The following free body describes the the satisfaction of force and moment equilibrium:



A force and moment balance of this configuration provides results for P_0 and P_1 as

$$L = 201 \text{ in}$$

Use end-to-end value

$$P_0 := \frac{-2 \cdot F_{\text{impact}_{125}}}{L}$$

$$P_0 = -4.791 \times 10^4 \frac{\text{lbf}}{\text{in}}$$

$$P_1 := \frac{4 \cdot F_{\text{impact}_{125}}}{L}$$

$$P_1 = 9.582 \times 10^4 \frac{\text{lbf}}{\text{in}}$$

The inertia induced pressure distribution along the length is

$$p(x) := 6 \cdot \frac{F_{\text{impact}_{125}}}{L} \cdot \left(\frac{x}{L}\right) - 2 \cdot \frac{F_{\text{impact}_{125}}}{L}$$

The shear force $V(x)$ at any section is

$$F := F_{\text{impact}_{125}}$$

$$V(x) := 6 \cdot \frac{F}{L} \cdot \left(\frac{x^2}{2 \cdot L} \right) - 2 \cdot \frac{F}{L} \cdot x$$

Finally, the bending moment $M(x)$ at any section x is given as

$$M(x) := -6 \cdot \frac{F}{L} \cdot \left(\frac{x^3}{6 \cdot L} \right) + 2 \cdot \frac{F}{L} \cdot \left(\frac{x^2}{2} \right)$$

The location along the length where maximum bending moment occurs is obtained by locating the point of zero moment derivative with respect to x .

$$x_{\max} := 2 \cdot \frac{L}{3}$$

The value for the maximum bending moment is

$$M_{\max} := -6 \cdot \frac{F_{\text{impact}_{125}}}{L} \cdot \left(\frac{x_{\max}^3}{6 \cdot L} \right) + 2 \cdot \frac{F_{\text{impact}_{125}}}{L} \cdot \left(\frac{x_{\max}^2}{2} \right)$$

$$M_{\max} = 1.434 \times 10^8 \text{ in}\cdot\text{lbf}$$

The maximum value of the axial membrane stress in the outermost shell is

$$\sigma_{\text{axial}} := \frac{|M_{\max}| \cdot d_{125}}{2 \cdot I_{125}} \quad \sigma_{\text{axial}} = 1.906 \times 10^4 \text{ psi}$$

The safety factor on primary membrane stress for this Level D accident condition of storage event is

$$SF := \frac{S_{Ia}}{\sigma_{\text{axial}}} \quad SF = 2.085$$

Note that no dynamic amplification need be applied to axial stresses since the lowest natural frequency is well above the value where elastic amplification will occur regardless of the duration of impact.

For the 100 ton HI-TRAC

$$P0 := \frac{-2 \cdot F_{\text{impact_100}}}{L}$$

$$P0 = -3.813 \times 10^4 \frac{\text{lbf}}{\text{in}}$$

$$P1 := \frac{4 \cdot F_{\text{impact_100}}}{L}$$

$$P1 = 7.626 \times 10^4 \frac{\text{lbf}}{\text{in}}$$

The inertia induced pressure distribution along the length is

$$p(x) := 6 \cdot \frac{F_{\text{impact_100}}}{L} \cdot \left(\frac{x}{L}\right) - 2 \cdot \frac{F_{\text{impact_100}}}{L}$$

The shear force $V(x)$ at any section is $F := F_{\text{impact_100}}$

$$V(x) := 6 \cdot \frac{F}{L} \cdot \left(\frac{x^2}{2 \cdot L}\right) - 2 \cdot \frac{F}{L} \cdot x$$

Finally, the bending moment $M(x)$ at any section x is given as

$$M(x) := -6 \cdot \frac{F}{L} \cdot \left(\frac{x^3}{6 \cdot L}\right) + 2 \cdot \frac{F}{L} \cdot \left(\frac{x^2}{2}\right)$$

The location along the length where maximum bending moment occurs is obtained by locating the point of zero moment derivative with respect to x .

$$x_{\text{max}} := 2 \cdot \frac{L}{3}$$

The value for the maximum bending moment is

$$M_{\text{max}} := -6 \cdot \frac{F_{\text{impact_100}}}{L} \cdot \left(\frac{x_{\text{max}}^3}{6 \cdot L}\right) + 2 \cdot \frac{F_{\text{impact_100}}}{L} \cdot \left(\frac{x_{\text{max}}^2}{2}\right)$$

$$M_{\max} = 1.141 \times 10^8 \text{ in}\cdot\text{lbf}$$

The maximum value of the axial membrane stress in the outermost shell is

$$\sigma_{\text{axial}} := \frac{|M_{\max}| \cdot d_{100}}{2 \cdot I_{100}} \quad \sigma_{\text{axial}} = 1.577 \times 10^4 \text{ psi}$$

The safety factor on primary membrane stress for this Level D accident condition of storage event is

$$\text{SF} := \frac{S_a}{\sigma_{\text{axial}}} \quad \text{SF} = 2.52$$

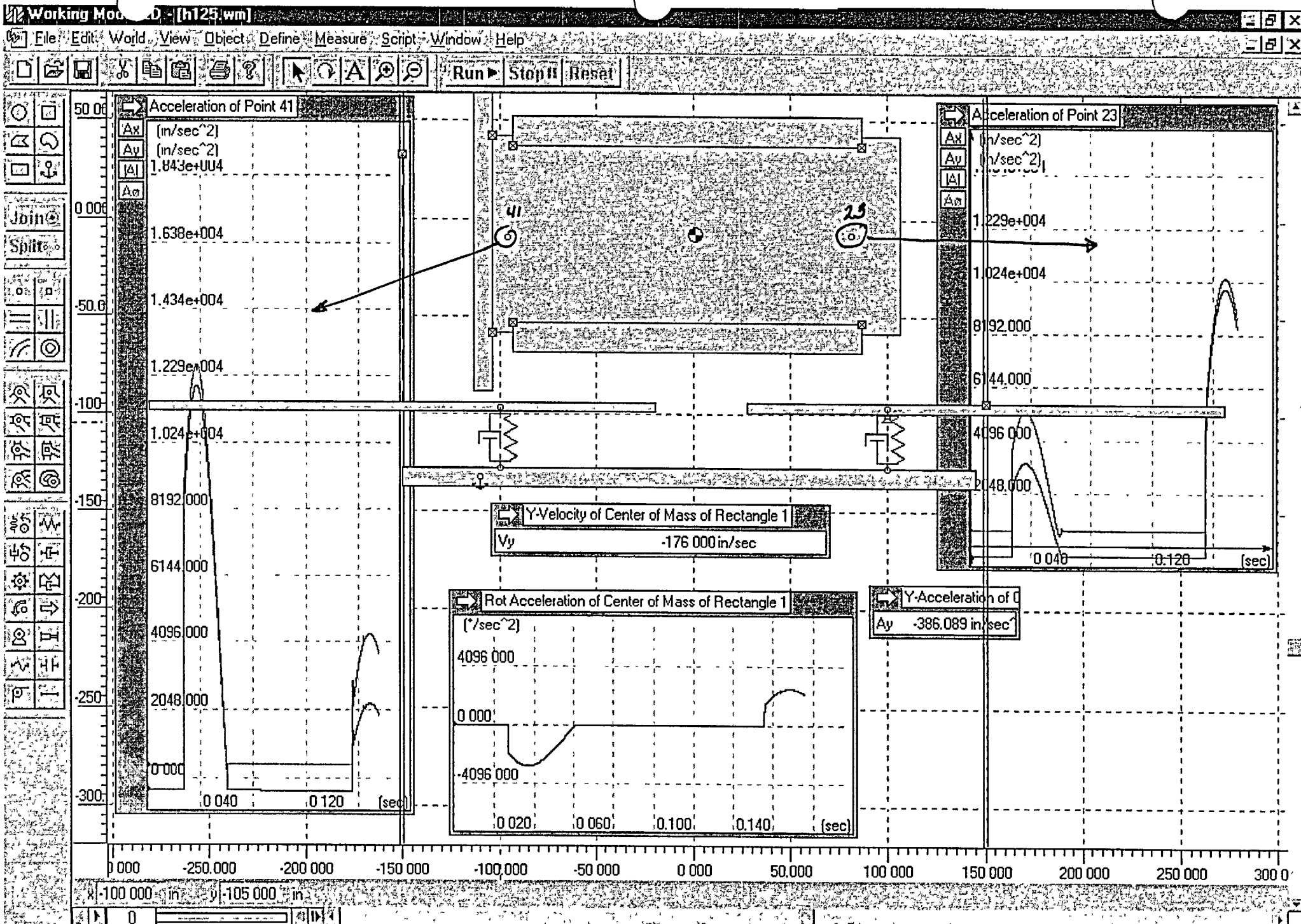
Note that no dynamic amplification need be applied to axial stresses since the lowest natural frequency is well above the value where elastic amplification will occur regardless of the duration of impact.

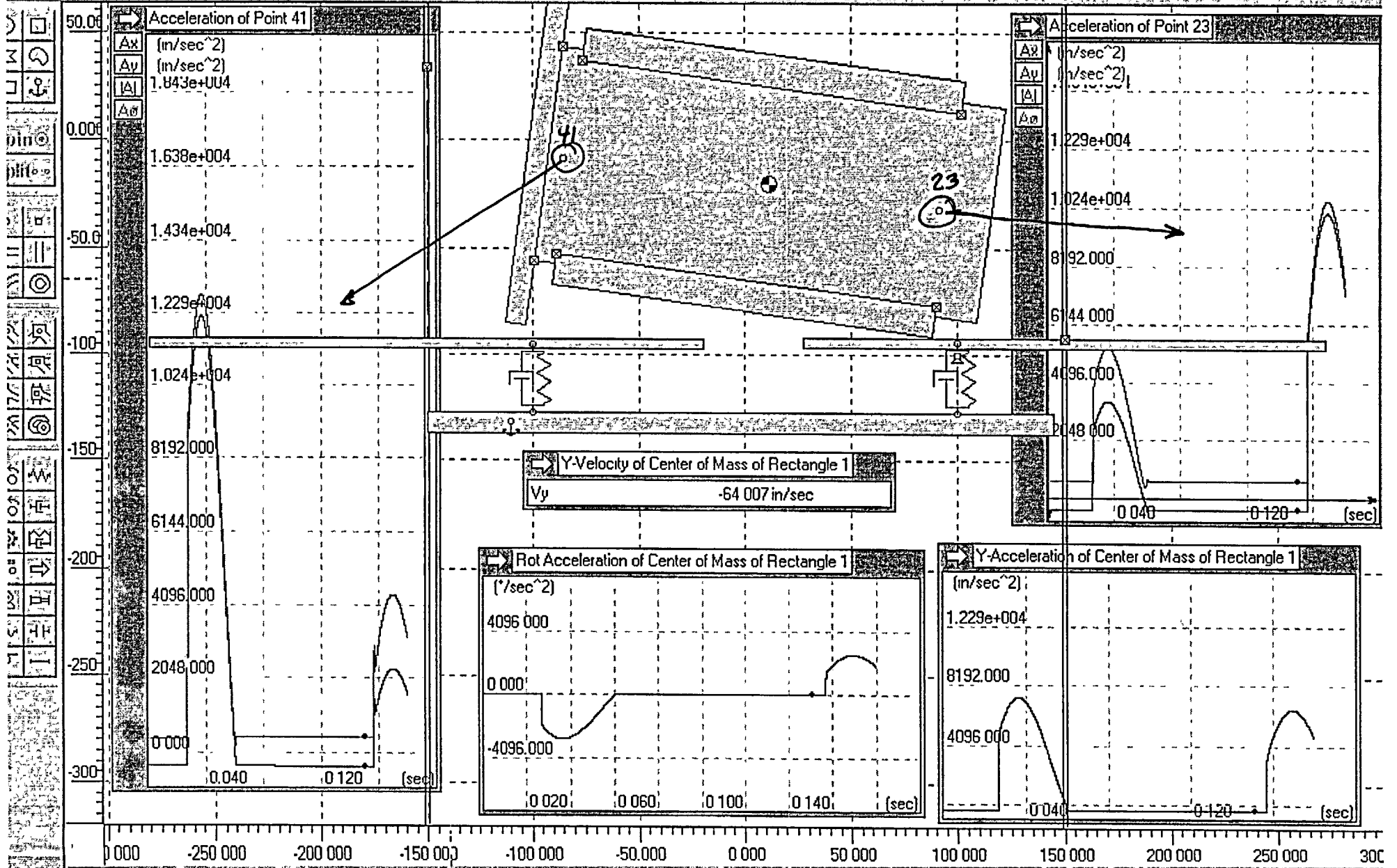
3.Z.13 Conclusions

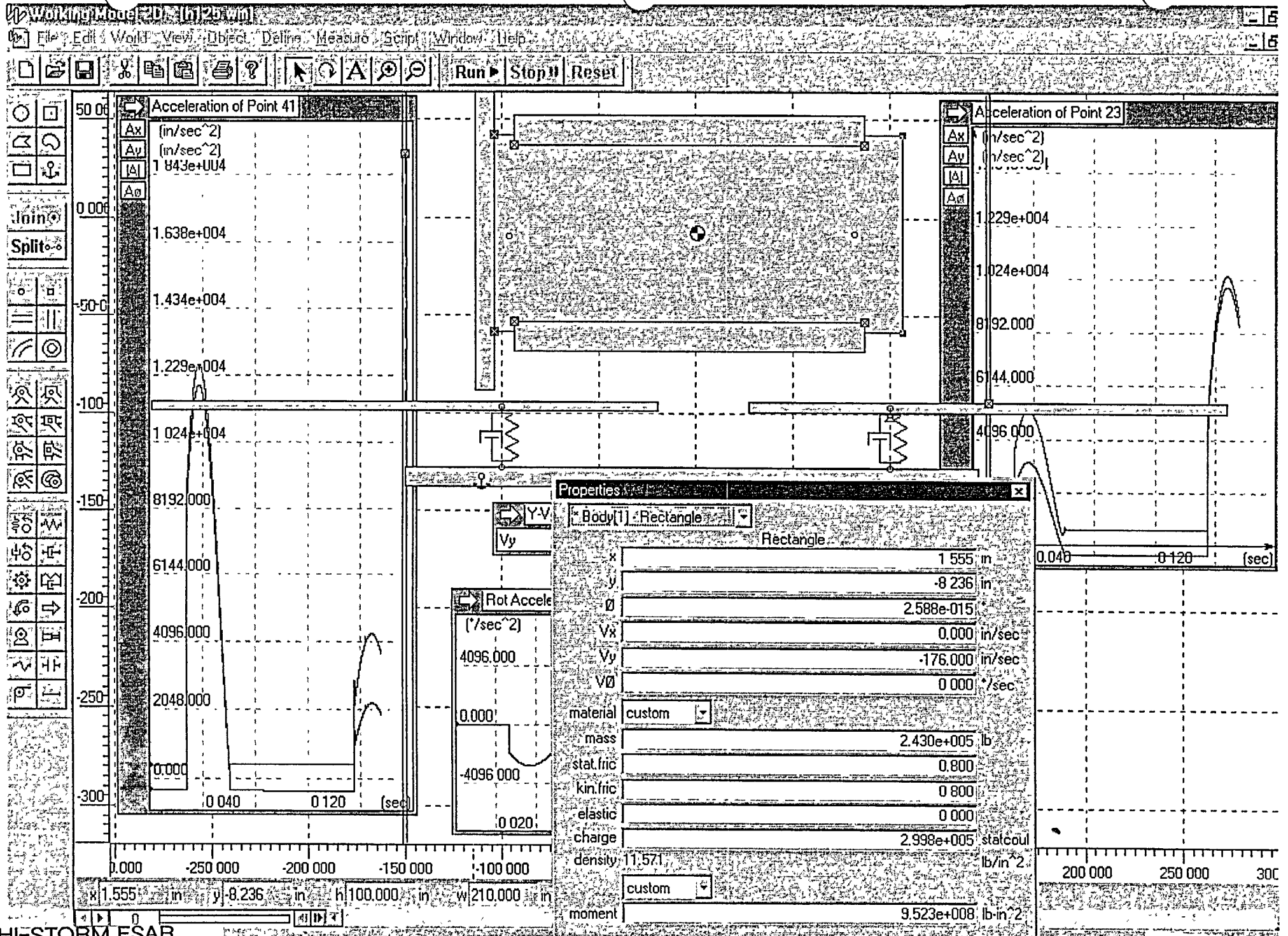
The HI-TRAC transfer casks have been evaluated for their performance under a drop accident starting from a given height above the target surface. The target surface has been defined by a simple spring damper system depending on the impact contact area (see Appendix 3.AL).

Deceleration levels resulting from the impacts are below the design basis of 45g's

Beam bending stress in the vessel is below yield and provides a comfortable margin against the allowable stress for this Level D event.







HI-STORM FSAR
HI-2002444

Fig. 3.Z.3 HI-TRAC 125 Mass Properties

Rev. 0

Properties

x	1.555
y	-8.236
z	-8.236
ρ	2.588e-015
V _x	0.000
V _y	-1.76000
V _z	0.000
material	custom
mass	2.010e+005
stat fitc	0.800
kin fitc	0.800
elastic	0.000
charge	2.998e+005
density	9.571
moment	7.807e+008

Rot Accele

(/sec^2)	0.000
	4.096000
	-4.096000
	0.020

Acceleration of Point 41

(m/sec^2)	1.843e+004
	1.638e+004
	1.434e+004
	1.229e+004
	1.024e+004
	8.192000
	6.144000
	4.096000

Acceleration of Point 23

(m/sec^2)	0.000
	0.040
	-0.120

Number of Mass of Rectangle 1

(sec)	0.000
	0.120

Fig. 3.Z.5 HI-TRAC Lower Impact Spring

